



David Publishing Company  
www.davidpublisher.com

ISSN 2162-5298 (Print)  
ISSN 2162-5301 (Online)  
DOI:10.17265/2162-5298

# Journal of **Environmental Science** and **Engineering A**

Volume 6, Number 8, August 2017



From Knowledge to Wisdom

# **Journal of Environmental Science and Engineering A**

Volume 6, Number 8, August 2017 (Serial Number 62)



David Publishing Company  
[www.davidpublisher.com](http://www.davidpublisher.com)

**Publication Information:**

*Journal of Environmental Science and Engineering A* (formerly parts of Journal of Environmental Science and Engineering ISSN 1934-8932, USA) is published monthly in hard copy (ISSN 2162-5298) and online (ISSN 2162-5301) by David Publishing Company located at 616 Corporate Way, Suite 2-4876, Valley Cottage, NY 10989, USA.

**Aims and Scope:**

*Journal of Environmental Science and Engineering A*, a monthly professional academic journal, covers all sorts of researches on environmental management and assessment, environmental monitoring, atmospheric environment, aquatic environment and municipal solid waste, etc..

**Editorial Board Members:**

Dr. Geanina Birescu (Romania), Dr. Balasubramanian Sellamuthu (Canada), Assistant Prof. Mark Eric Benbow (USA), Dr. Khaled Habib (USA), Dr. Satinder Kaur Brar (Canada), Dr. Sergey Kirpotin (Russia), Dr. Ali Noorzad (Iran), Dr. Bo Richter Larsen (Italy), Dr. Mohamed Abu-Zeid El-Nahrawy (Egypt), Prof. Anton Alexandru Ciucu (Romania), Associate Prof. Hideki Kuramitz (Japan), Prof. N. Rama Swamy (India), Dr. Bisheng Wu (Australia).

Manuscripts and correspondence are invited for publication. You can submit your papers via Web Submission, or E-mail to [environmental@davidpublishing.org](mailto:environmental@davidpublishing.org), [environmental@davidpublishing.com](mailto:environmental@davidpublishing.com) or [info@davidpublishing.com](mailto:info@davidpublishing.com). Submission guidelines and Web Submission system are available at <http://www.davidpublisher.com>.

**Editorial Office:**

616 Corporate Way, Suite 2-4876, Valley Cottage, NY 10989, USA

Tel: 1-323-984-7526, 323-410-1082

Fax: 1-323-984-7374, 323-908-0457

E-mail: [environmental@davidpublishing.org](mailto:environmental@davidpublishing.org); [environmental@davidpublishing.com](mailto:environmental@davidpublishing.com); [info@davidpublishing.com](mailto:info@davidpublishing.com)

Copyright©2017 by David Publishing Company and individual contributors. All rights reserved. David Publishing Company holds the exclusive copyright of all the contents of this journal. In accordance with the international convention, no part of this journal may be reproduced or transmitted by any media or publishing organs (including various websites) without the written permission of the copyright holder. Otherwise, any conduct would be considered as the violation of the copyright. The contents of this journal are available for any citation. However, all the citations should be clearly indicated with the title of this journal, serial number and the name of the author.

**Abstracted/Indexed in:**

Googel Scholar

CAS (Chemical Abstracts Service)

Database of EBSCO, Massachusetts, USA

Chinese Database of CEPS, Airiti Inc. & OCLC

Cambridge Science Abstracts (CSA)

Ulrich's Periodicals Directory

Chinese Scientific Journals Database, VIP Corporation, Chongqing, China

Summon Serials Solutions

ProQuest

**Subscription Information:**

Price (per year):

Print \$600, Online \$480

Print and Online \$800

David Publishing Company

616 Corporate Way, Suite 2-4876, Valley Cottage, NY 10989, USA

Tel: 1-323-984-7526, 323-410-1082; Fax: 1-323-984-7374, 323-908-0457

E-mail: [order@davidpublishing.com](mailto:order@davidpublishing.com)

Digital Cooperative Company: [www.bookan.com.cn](http://www.bookan.com.cn)



David Publishing Company  
[www.davidpublisher.com](http://www.davidpublisher.com)

# Journal of Environmental Science and Engineering A

Volume 6, Number 8, August 2017 (Serial Number 62)

## Contents

### Water Environment

- 381 **Assessment of Salinization in the Main River Systems of Long An Province, Vietnam**  
*Can Thu Van, Nguyen Thi Tuyet, Do Thi Hong Hoa, Can The Viet, Do Mien and Nguyen Van Hieu*

### Environmental Chemistry

- 388 **Recovery of Copper and Cobalt from Copper Slags as Selective**  
*Uyan Yuksel, Ibrahim Tegin and Recep Ziyadanogullari*

### Environmental Biology

- 395 **Evaluation of Pb, Cu, Zn and Cd Levels in Some Plants at Roadsides between Mafraq and Jerash, Jordan**  
*Abdullah Trad Al-fawwaz and Khaled Abdu Al-Khazaleh*

### Environmental Material

- 402 **Eco-friendly Leather: Chromium Reduction in the Tanning Cycle**  
*Elena Salernitano, Alessandra Strafella, Mercedes Roig and Alice Dall'Ara*
- 410 **Fluorescence Properties of the Lanthanide Supported onto Titanate Nanosheets**  
*Daisuke Yoshioka, Yasumitsu Nishimura and Ken-ichi Katsumata*
- 415 **The Introduction of Biofuels in Marine Sector**  
*Theodora Tyrovola, George Dodos, Stamatis Kalligeros and Fanourios Zannikos*

### Environmental Economics

- 422 **Economic Analysis of the Internalization the Externalities in Environmental Goods**  
*Odyseas Kopsidas and Andreas Hadjixenofontos*

# Assessment of Salinization in the Main River Systems of Long An Province, Vietnam

Can Thu Van<sup>1</sup>, Nguyen Thi Tuyet<sup>1</sup>, Do Thi Hong Hoa<sup>1</sup>, Can The Viet<sup>2</sup>, Do Mien<sup>3</sup> and Nguyen Van Hieu<sup>4</sup>

1. *Hochiminh City University of Natural Resources and Environment, Ho Chi Minh City 700000, Vietnam*

2. *Thang Long Joint Stock Company, Ho Chi Minh City 700000, Vietnam*

3. *Hydro-Meteorological Center of Long An Province, Tan An City 850000, Vietnam*

4. *Ministry of Natural Resources and Environment, Ha Noi 100000, Vietnam*

**Abstract:** Three provinces including Long An, Tien Giang and Dong Thap, located at Dong Thap Muoi area in the Mekong Delta, belong to the southern key economic region of Vietnam. These provinces run from west to east with a vast network of rivers. Among them, VCD (Vam Co Dong), VCT (Vam Co Tay) and Soai Rap rivers are the three biggest rivers crossing the province. In recent years, the flows of rivers have changed a lot and saline intrusion has been very complicated. Salt water has intruded deeply into the field. In the 2000s, salt water only reached Tuyen Nhon (Thanh Hoa district), but now it has reached Vinh Hung district, about 50 km far from Tuyen Nhon. In 2016, the maximum of salinity in Xuan Khanh (Duc Hoa district) in VCD river was 6.8‰ and Tuyen Nhon (Thanh Hoa district) in VCT river was 5.2‰. In the coming years, the situation of salt intrusion is going to happen more unpredictable under effects of global climate change and sea level rise.

**Key words:** Salinization, Vam Co river system, LA (Long An) province.

## 1. Introduction

### 1.1 Natural Condition in LA (Long An) Province

LA is a province in the southern region of Vietnam, 50 km far from the center of Ho Chi Minh city, bordered by Svay Rieng province (Cambodia) in the north, Tien Giang province in the south and Tay Ninh province and Ho Chi Minh city in the east (Fig. 1). The province runs mostly from west to east with a vast network of rivers. Among them, VCD (Vam Co Dong), VCT (Vam Co Tay) and Soai Rap rivers are the three biggest rivers crossing the province for waterway transport and agriculture [1, 2].

#### 1.1.1 Geographic Location

LA province with area of 449,194.49 ha and population of 1,542,606 has a rather special geographic location in the Mekong Delta, belonging

to the southern key economic development zone. It is defined as a dynamic economic region that plays an important role in the economic development strategy of Vietnam [1, 2].

#### 1.1.2 Topography

The topography of LA province is relatively flat with elevation ranging from 0.5 m to 1.0 m, except for 2.0 m and 3.0 m in the border area between Vietnam and Cambodia and up to 4 m in some areas of Duc Hoa. In general, the terrain of LA province slopes from northwest to southeast [1, 3].

#### 1.1.3 Climate

LA has high, quite stable temperature and humidity throughout the year. The proportion of annual evaporation is quite high and distinct seasonal variation. There are two types of monsoons prevalent in the year: the northeast monsoon from November to April and the southwest monsoon from May to October. LA is one of the provinces in the Mekong Delta with low annual rainfall varying from 1,600 to 1,740 mm/year [4, 5].

---

**Corresponding author:** Can Thu Van, Ph.D., main research field: hydrology and waterresources.

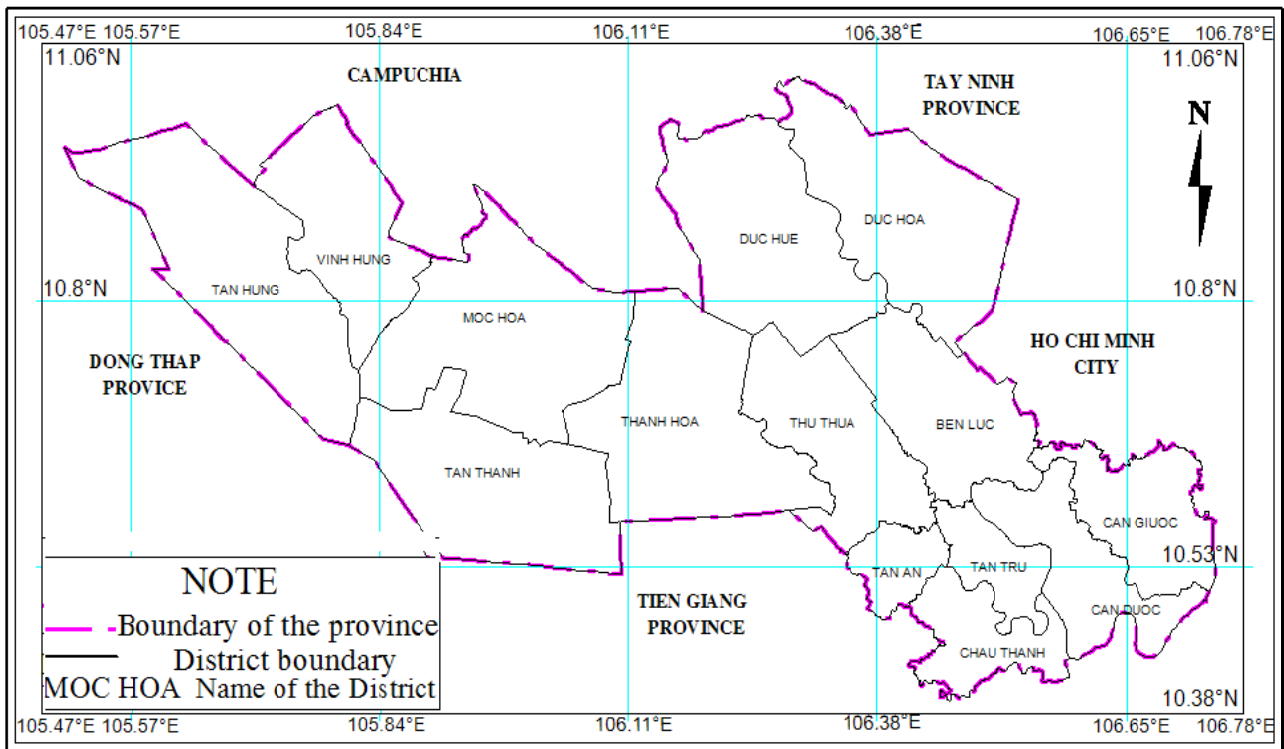


Fig. 1 The map of Long An province [1].

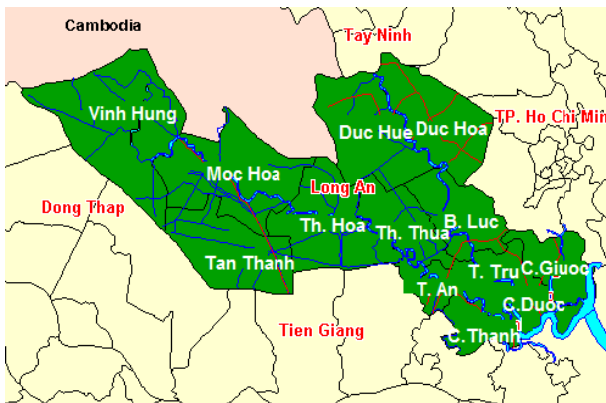


Fig. 2 The river system in Long An province [1].

1.1.4 The River System (Fig. 2)

VCT river with 235 km length originates from Svayri (Cambodia), flows through Binh Tu, Binh Chau to VCT river and joins with Vam Co river, and pours into the East Sea at Soai Rap.

VCD river with 278 km length originates from Cambodia, flows through Xa Mat to Go Dau (Tay Ninh province) and enters Vam Co river and flows into the East Sea.

Cai Cai is a natural canal, connecting with the

Trabek (Cambodia) river to the center of Dong Thap Muoi region. This canal with about 100 m width and 8-10 m depth is also a boundary between Dong Thap and LA province. In the flood season, a large amount of water from Cambodia comes to LA through this canal.

Internal canal system includes the canals connect with two rivers VCT and VCD with 70 km length. The canals connecting the Tien river to VCT river are the main sources supplying freshwater in the flood and dry season from the Tien river to the Dong Thap Muoi region through the VCT river. The other canals connecting the Mekong river to the Saigon river are quite shallow and the water level is completely fluctuated by tide.

1.2 The Flows and Tidal Water Level in LA Province

1.2.1 The Flow

The flood season in LA is from August to December (5 months) in the west-northwest. In the south-southeast, floods usually appear later with lower water level.

Every year, the flood in the Mekong river overflows the Dong Thap Muoi region and VCT river. This leads to water level of VCT river always higher than that of VCD river. Therefore, the flood flows from VCT river to VCD river and from VCD river flows to the southwest area of Ho Chi Minh city.

At present, the system of embankments and dikes in this area has been developed and controlled the flood flow very well. Thus, the flows with low water level will go from VCT river to the VCD river through the canals. On the other hand, the flows with high water level will overflow the dike system to the VCD river [6].

### 1.2.2 The Tide

The rivers and canals in LA province were affected by the irregular semi-diurnal tidal regime of the East Sea with high tidal range (about 300 ÷ 350 cm). Foot tidal water level is about 160 ÷ 300 cm and peak tidal water level is approximately 80 ÷ 100 cm. As a result, the maintaining duration of high water level is longer than that of low water level and the daily mean water level is as high as the tide peak [2].

In LA province, changes in extreme weather make the characteristics of the flow unpredictable (Fig. 3).

In Moc Hoa district (northwest area), the annual rainfall decreases, especially in the dry season. This causes drought, water shortage and salt intrusion more strictly.

The data measured in LA coastal station show that high tide combined with big waves has caused landslides and salt intrusion into the field in recent years. This affects on socio-economic development. The data from 1984 to 2014 indicate that high tide levels are from September to December each year and the tidal range varies from 0.70 m to 1.00 m. The lowest water level is from March to August every year and the tidal range varies from 2.45 m to 2.50 m. The tidal range in the dry season is greater than that of the flood season.

From 2010 to 2014, the tide water level changed complicatedly. In the dry season (February-April), the increased water level at tidal peak and tidal foot,

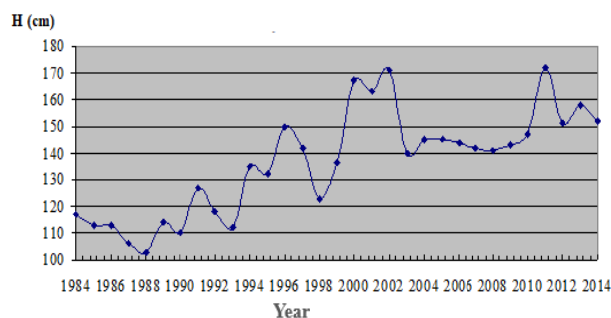


Fig. 3 Yearly maximum water level in Tan An [2].

more and more intense wind, strong sun, as well as high temperature cause serious salt intrusion into the field.

At the Soai Rap estuary, the irregular semi-diurnal tidal regime of the East Sea, the tide time per day is 24 hours 50 minutes and a tide period is 13-14 days. The peak tidal range reaches 235 cm at Tan An and 85 cm at Moc Hoa. The southern districts are affected the most by the salt intrusion, about 4 to 6 months each year [6].

## 2. Material and Methods

The research methods used in this study include: collecting, analyzing documents from existing sources, surveying field, sampling and analyzing samples at river monitoring stations to assess salt intrusion. Then, it is necessary to apply the mathematical modeling method to simulate hydraulic, hydrological regime and water quality in the main river system in LA province [7, 8].

Hydraulic module is developed from the one dimensional Saint Venant equation for unstable flows, expressed by Eqs. (1) and (2) [8, 9]:

Continuity equation:

$$\frac{\partial Q}{\partial x} + \frac{\partial A}{\partial t} = q \quad (1)$$

Momentum equation:

$$\frac{\partial Q}{\partial t} + \frac{\partial \left( \alpha \frac{Q^2}{A} \right)}{\partial x} + g \cdot A \cdot \frac{\partial h}{\partial x} + \frac{gQ|Q|}{c^2 \cdot A \cdot R} = 0 \quad (2)$$

Advection-Dispersion module is used to simulate the one dimensional transport of suspended solids or dissolved compound in open channel, based on the

equation for cumulative storage assuming that these substances are dissolved and mixed. This process is represented by Eq. (3) [8, 9]:

Diffusion equation:

$$\frac{\partial AC}{\partial t} + \frac{\partial QC}{\partial x} - \frac{\partial}{\partial x} \left( A \cdot D \cdot \frac{\partial C}{\partial x} \right) = -A \cdot K \cdot C + C_2 Q \quad (3)$$

Ecological module is included with the advection-dispersion module. This means that the ecological module calculates the bioremediation processes of the compounds in the river while the advection-dispersion module is used to simulate the transport and diffusion of the compounds [8, 9].

In which  $Q$ : flow rate ( $m^3/s$ );  $A$ : cross section area ( $m^2$ );  $x$ : length (m);  $t$ : time (s);  $R$ : hydraulic radius (m);  $h$ : water depth (m);  $g$ : gravity acceleration ( $m^2/s$ );  $C$ : concentration of dissolved compound (g/L);  $K$ : linear decay coefficient;  $\alpha$ : dynamical correction coefficient;  $D$ : diffusion coefficient ( $m^2/s$ ); and  $C_2$ : concentration of input streams [8, 9].

### 3. Results and Discussion

The process of establishing, calibrating and verifying the model and hydrodynamic simulation results is presented by Can, T. V. and Nguyen, T. S. [8].

Results of analysis, calculation and simulation of salinity were determined at Tan An, Ben Luc, Cau Noi, Xuan Khanh and Tuyen Nhon stations, which is shown in Fig. 4, in the dry season from February to July (the lowest period) from 2005 to 2016 as Figs. 5-9.

The basic data of actual measurements and simulations of salinity in the dry season several years showed that the highest salinity was reached in March, April and May. That is because the water volume from the Mekong river upstream flow through Tan Chau

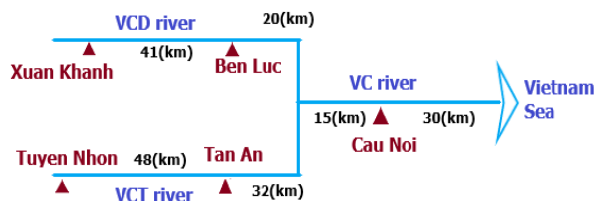


Fig. 4 The main river system and simulation locations.

(Tien river) to the VCT in the dry season was a very small amount. Moreover, precipitation amount is not available or very little at that time, and the water volume in rivers' downstream was being reduced, leading to that result that the East Sea tide has been more and more intruded into the delta.

#### 3.1 At Cau Noi Station (Called My Loi Bridge) (Fig. 5)

This location is about 30 km far from the Soai Rap river estuary of Vam Co river in LA province, therefore this area has been impacted by the East Sea tide and the salinity is the highest in the simulated

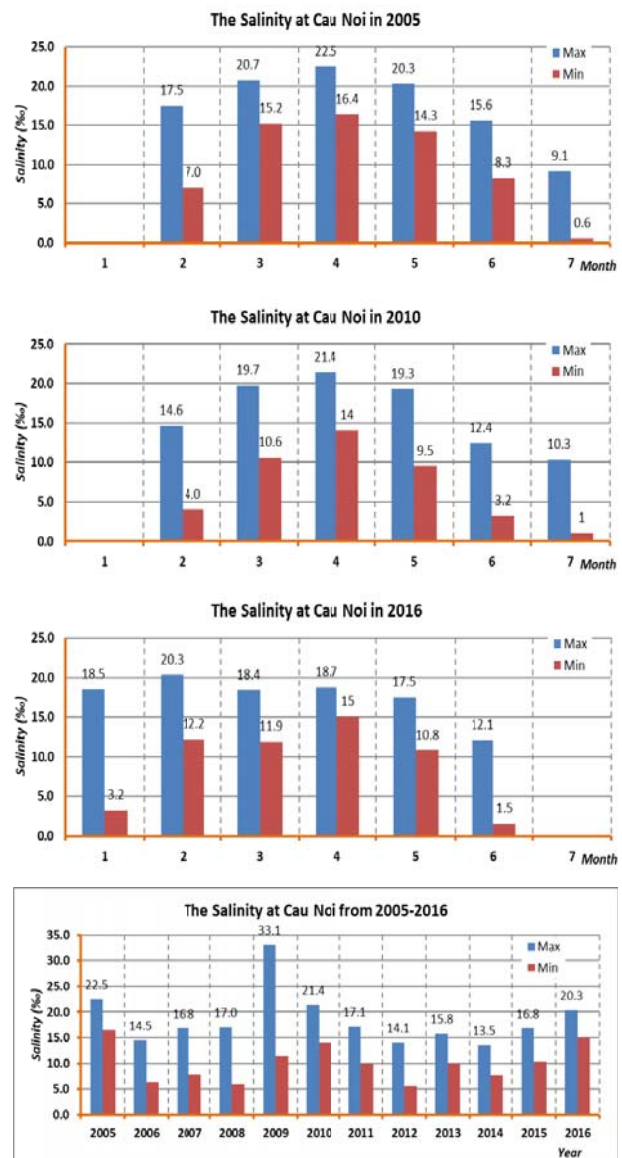


Fig. 5 The salinity at Cau Noi station (Vam Co river).

locations. This located at nearby the river estuary, so this has been only lightly impacted by Mekong upstream, thus the salinity at Cau Noi was not hardly effected by the amount of water volume in the dry season flows to Tan Chau. The highest salinity in the Cau Noi was 33.1‰ in July 2009 and other months in dry season in 2009 showed the salinity also was more higher than 10‰. At here, in 2005, 2010 and 2016, the highest salinity was over 20‰ and lowest salinity was 14‰, especially in 2016 the salinity of the dry season was over 17.5‰.

3.2 At Ben Luc Station (Fig. 6)

Ben Luc is the location in VCD river and is the location where measured the salinity from the East

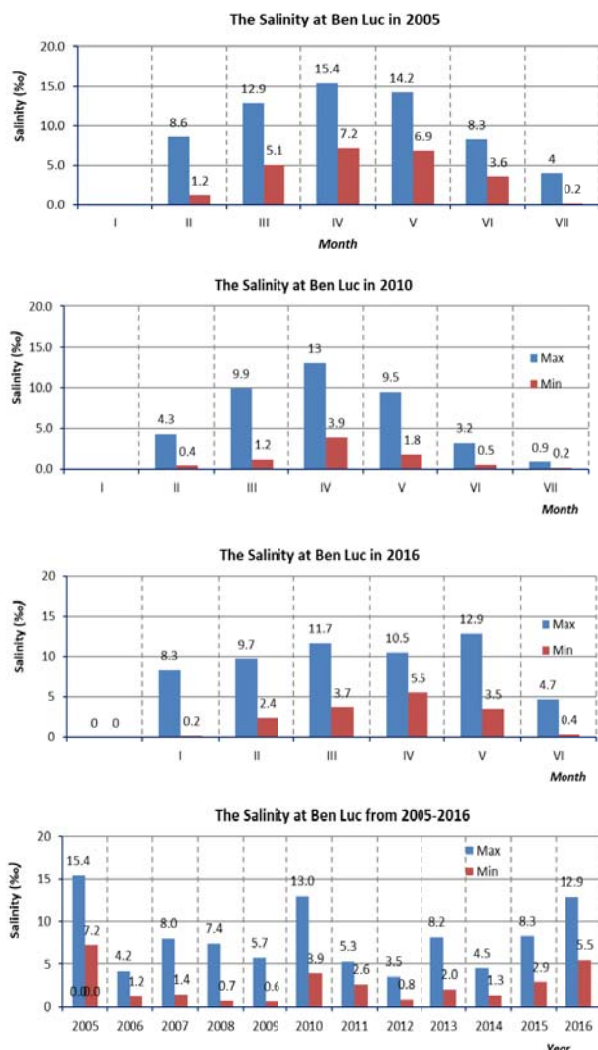


Fig. 6 The salinity at Ben Luc station (VCD river).

Sea intruding into the VCD river through the Vam Co river and the distance from Ben Luc to the estuary is about 64 km and about 34 km to Cau Noi station. The salinity was highest at 15.4‰ in May 2005 and in other months from February to June 2005 also reached 8.3‰ to 14.2‰. The salinity in 2010 was the highest at 13.0‰ and at 12.9‰ in 2016. Except for the years 2005, 2010 and 2016 with high salinity, the other years in that time there was a low salinity. From 2006 to 2009, the highest salinity in the months of the year in Ben Luc was continuously decreased and the lowest was 4.2‰ in 2006 and 5.7‰ in 2009, especially the lowest salinity in 2009 was only 0.6‰. From 2011 to 2015, the highest salinity was in the range of 3.5‰ in 2012 to 8.2‰ in 2013, and the lowest salinity of the year was 0.8‰ in 2012. Especially in 2005, 2010 and 2016, the salinity in Ben Luc was high in 4 months from February to May with salinity over 9‰. In period 2005-2016, the lowest salinity in Ben Luc was 3.5‰ in 2012.

3.3 At Tan An Station (Fig. 7)

This site locating at the VCT river, helps to measure the salinity from the sea intruded into the Vam Co river. Tan An is about 77 km from Soai Rap estuary and about 47 km from Cau Noi station. The same as Ben Luc station, Tan An station also recorded in three years 2005, 2010 and 2016 with high salinity. The highest salinity was 15.7‰ in April and May 2005, was 11.2‰ in April and May of 2010, and reached 11.7‰ in 2016, conversely the salinity was lower than 7‰ in other years. In Tan An, the years of salinity were divided in three groups: (i) over 11‰ in 2005, 2010 and 2016; (ii) 7-8‰ in 2007, 2008, 2013 and 2015; (iii) under 3‰ in 2006, 2009, 2011, 2012 and 2014; even in 2012, the highest salinity was only 0.7‰ (almost not affected salinity).

3.4 At Xuan Khanh Station (Fig. 8)

This station is about 106 km from Soai Rap estuary and about 41 km from Ben Luc. The salinity was remarkable only in the dry season in the years of 2005,

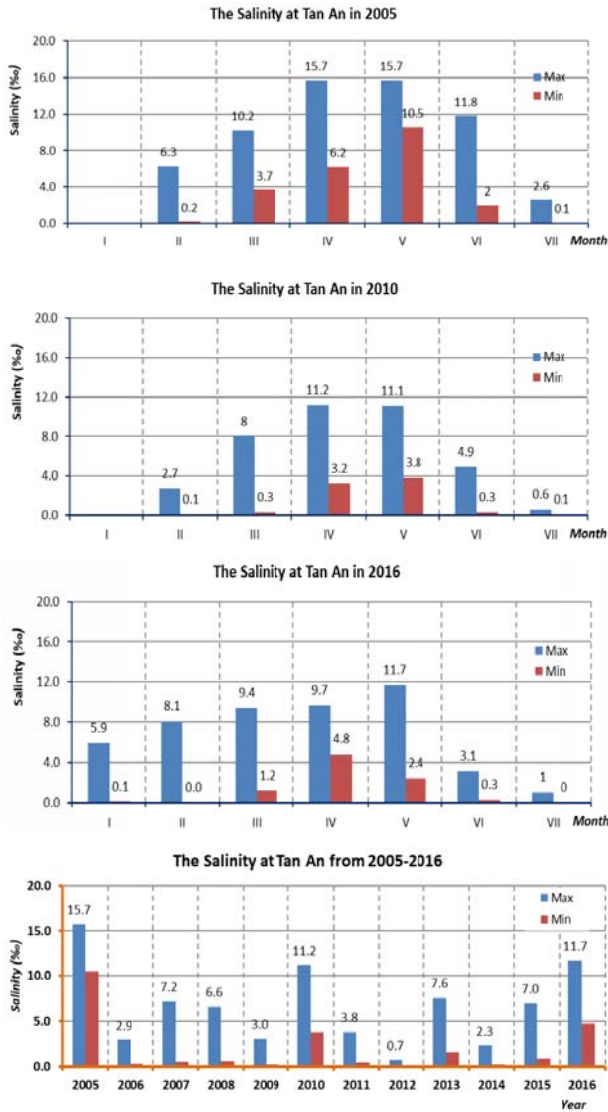


Fig. 7 The salinity at Tan An station (VCT river).

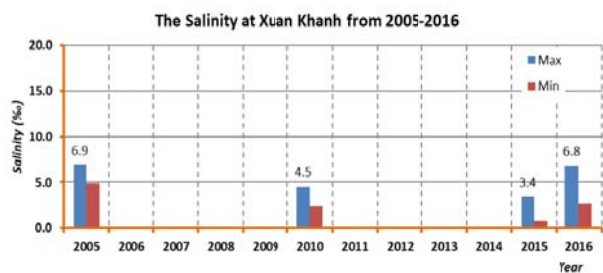


Fig. 8 The salinity at Xuan Khanh station (VCD river).

2010, 2015 and 2016. Especially in 2005 and 2016, the driest season happened and then there was a serious shortage of water, and the salinity was up to 6.9‰ in 2005 and 6.8‰ in 2016. The salinity was in the range of 3-4.5‰ in the years of 2010 and 2015 but only two months each year.

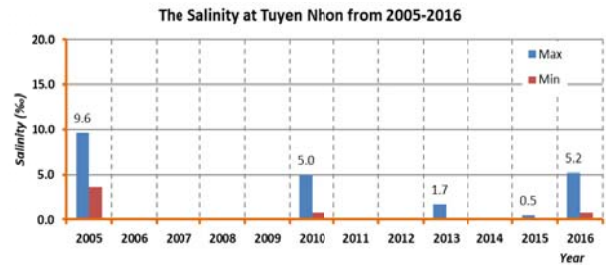


Fig. 9 The salinity at Tuyen Nhon station (VCT river).

### 3.5 At Tuyen Nhon Station (Fig. 9)

Tuyen Nhon located in the upstream of VCT and is about 48 km from Tan An in VCT river and 115 km from Soai Rap estuary. As the same Xuan Khanh station, the salinity here was only remarkable in the flood season with low water in the years of 2005, 2010 and 2016. Especially in 2005, the highest salinity was 9.6‰ in April and May, and the salinity was 5.2‰ in 2 months of the year 2016.

## 4. Conclusions

The collection, calculation and simulation at locations on the main river system in LA such as VCD river, VCT river and Vam Co river showed that salinity was very fluctuated unpredictably. The salinity in the river system in LA was influenced by the upstream flow of the Mekong river and the tidal regime of the East Sea.

Moreover, In the coming years, the situation of salt intrusion is going to happen more unpredictably under effects of global climate change and sea level rise.

## Acknowledgement

The paper was a part of the scientific results in the Ministerial-Level Research Project (Ministry of Natural Resources and Environment), code TNMT2016.05.10. The authors are grateful to be supported on the finance and human resources by Ministry of Natural Resources and Environment and Ho Chi Minh City University of Natural Resources and Environment.

## References

[1] Long An Information Portal. 2013. "Introduction of Natural Conditions in Long An Province." Accessed

- October 7, 2013. <http://www.longan.gov.vn>.
- [2] Department of Statistics of Long An Province. 2016. *Long An Province Statistical Yearbook*. Yearly report, Socio-economic Summation of Long An Province.
- [3] Luong, Q. X. 2012. *Master Plan Irrigation in Mekong Delta in Condition of Climate Change and Rising Sea Level*. Final report, Southern Institute of Water Resources Planning,
- [4] Sam, L. 2007. *Research Results of Salinity Intrusion for Socio-economic Mekong Delta*. Final report, Southern Institute of Water Resources Research.
- [5] Hoanh, C. T., Guttman, H., Droogers, P., and Aerts, J. 2003. "Water, Climate, Food and Environment in the Mekong Basin in South Asia." *Final Report to the ADAPT Project, Adaptation Strategies to Changing Environments*. International Water Management Institute, Mekong River Commission Secretariat, Institute of Environmental Studies.
- [6] Tuan, D. N., Phung, K. N., Loi, K. N., Van, T. C., Truong, D. C., Khanh, T. N., et al. 2014. *Research and Development of Decision Support System for Land and Water Resource Management in the Mekong Delta Responding to Climate Change*. Final report Project of Government Level.
- [7] Lam, M. P., Van, P. D. T., and Tran, Q. D. 2013, "Application of One-dimensional Hydrodynamic Model to Assess the Historical Saline Intrusion Dynamics and to Predict the Future Dynamics in the Main River Network in the Tra Vinh Province." *Can Tho University Scientific Journal* 25 (A): 68-75.
- [8] Can, T. V., and Nguyen, T. S. 2016. "Simulation of Hydrological, Hydraulics in Mekong Delta to Assess the Impact of the Dike System to Change the Flow in Dong Thap Muoi." *Vietnam University National Scientific Journal* 32 (3S): 256-63.
- [9] DHI (Denmark Hydraulic Institute). 2007. "A Modelling System for River and Channels-Mike 11." *User Manual Book*. Danmark: DHI Software, Water and Environment.

# Recovery of Copper and Cobalt from Copper Slags as Selective

Uyan Yuksel<sup>1</sup>, Ibrahim Tegin<sup>2</sup> and Recep Ziyadanogullari<sup>3</sup>

1. Department of Chemistry, Vocational School of Technical Sciences, Siirt University, Siirt 56100, Turkey

2. Department of Chemistry, Faculty of Science and Art, Siirt University, Siirt 56100, Turkey

3. Department of Chemistry, Faculty of Science, Dicle University, Diyarbakır 21280, Turkey

**Abstract:** This study focuses on the recovery of copper and cobalt from copper slags obtained from Kure district of Kastamonu city, which is in the north of Turkey, and removal of Se, Te, Sb and As from mixture of copper slag and copper concentrate has been conducted. Homogeneous mixtures of slag/pyrite/copper concentrate rate were subjected to roasting at high temperatures in a closed medium and then it was processed roasting at air atmosphere at 600 °C. In the leaching experiments, the effects of roasting time, rate of slag/pyrite/copper concentrate and the effect of the added iron powder to leaching on the metals dissolution were investigated. Under optimum conditions, 99.6% of copper and 98.4% of cobalt were extracted in roasting at high temperatures in a closed medium 3:6:6 of slag/pyrite/copper concentrate rate then roasting at 600 °C at 5 hours. Besides, it was determined that all of Se, Te, Sb and As can be removed from the mixture of slag/pyrite/copper concentrate rate.

**Key words:** Copper, cobalt, slag, roasting, pyrite, copper concentrate.

## 1. Introduction

Significant amounts of copper, cobalt and nickel can be obtained from copper slags, which are produced in the thousands of tons per year in copper smelters. Very different methods were used to recover metals from the copper converter slags. Hydrometallurgical treatment of the slag, including direct leaching in sulfuric acid [1], leaching in sulfuric acid through H<sub>2</sub>S gas [2, 3], or ferric chloride [4], was proposed. Roasting of the slag with sulfuric acid, ammonium sulphate [5], ferric sulphate [6], or in reduction conditions [7], followed by acidic leaching, was reported in the literature. Bese, A. V. [8] investigated the effect of ultrasonic energy on the dissolution of copper from copper converter slag. The effects of parameters such as temperature, acid concentration, ferric sulphate concentration and time were also studied. The extraction efficiency of copper,

zinc, cobalt and iron from slag were 89.28%, 51.32%, 69.87% and 13.73%, respectively. A new hydrometallurgical method was developed to selectively extract base metal values, such as cobalt, zinc and copper from copper smelter slag at atmospheric pressure [9]. Roasting of the slag with sulfuric acid [10] has metal values in solution. In the leaching experiments, the effects of roasting time, acid/slag ratio, roasting temperature and application of thermal decomposition prior to leaching on the metals dissolution extents were investigated. 88% of copper, 87% of cobalt, 93% of zinc and 83% of iron were extracted in 2 h of roasting at 150 °C and 3:1 acid/slag ratio. A method was developed [11] to obtain copper and cobalt from oxidized copper ore and converter slag.

This study deals with the issues related to the recovery of Cu and Co from copper slag obtained from Kastamonu Kure region. Mixtures of copper slag, pyrite and copper concentrate were subjected to roasting at high temperature in a closed medium and then, they were roasted at 600 °C for different time

---

**Corresponding author:** Uyan Yuksel, Ph.D., main research fields: preconcentration, chromatography, spectroscopy and solid phase extraction.

intervals. By treatment with hot water, recovery of copper and cobalt from the ore mixture was aimed selectively.

## 2. Experiment

### 2.1 Sample Preparation

The slag sample used in this investigation is a composite from different levels of the copper slag obtained from Kastamonu Kure region, the chemical composition of which is given. A mineralogical study by Arslan, C. [12] showed that this slag usually has ferritic in nature, the appearance of bornite ( $\text{Cu}_5\text{FeS}_4$ ) and a metastable phase. The sample was crushed with a jawbreaker (Baysan Model) and grounded in a rotor beater mill (Retsch SRZ). The particle sizes of the samples were shifted to less than  $150\ \mu\text{m}$  and dried at  $105\ ^\circ\text{C}$  for one day. The chemical analysis of the slag sample is 1.00% Cu, 0.30% Co, 26.65% Fe and 1.1% S. Chemical analysis of the pyrite sample is 0.25% Cu, 0.24% Co, 43.00% Fe and 50.10% S. Chemical analysis of the copper concentrate sample is 18.25% Cu, 0.11% Co, 30.00% Fe and 42.50% S. 220 g samples of slag/pyrite/copper concentrate rate were subjected to roasting at high temperatures in a closed medium and then 10 g samples were finally processed roasting at air atmosphere at  $600\ ^\circ\text{C}$  at different times.

### 2.2 Digestion Procedure

Samples were digested by using the Berghof Speedwave MWS-3 model microwave digestion system. The microwave acid digestion was carried out as 0.2 g portion of the dried sample was weighed and transferred into a pressure-resistant PTFE (Polytetrafluoroethylene) vessel (volume 100 mL) and

the mixture of acids ( $\text{HNO}_3 + \text{HCl}$ , 2.5:7.5 mL) was added. Microwave digestion system under the conditions was described in Table 1. The power applied in program was 1,450 W. The reaction mixture was subjected to an evaporation module in order to remove the acids after the final digestion. Then the residue was dissolved in Milli-Q water and filtered, and the filtrate was diluted to a fixed volume.

### 2.3 Reagents and Instrumentation

The reagents used were of Suprapur® grade (Merck & Co., Darmstadt, Germany) when available or of analytical grade and used without further purification. Deionized water, obtained with a Milli-Q™ system (Millipore Corporation, Bedford, MA, USA), was used throughout this study. Stock standard solutions of Cu, Co, Se, Te, Sb, As and S at a concentration of 1,000 mg/L were purchased from E. Merck, Darmstadt, Germany. Nitric acid ( $\text{HNO}_3$ , 65%), hydrochloric acid ( $\text{HCl}$ , 37%), iron powder and hydrogen peroxide ( $\text{H}_2\text{O}_2$ , 30%) were analytical grade reagents.

Model Optima™ 7000 DV ICP-OES (Inductively Coupled Plasma Optical Emission Spectrometer) (PerkinElmer, Inc., Shelton, CT, USA) was used to determine the quantities of metal. The instrumental conditions were optimized to obtain sufficient sensitivity and precision Table 2.

The spectral wavelength selected for the metal analyses is shown in Table 3. The results are presented in Table 3.

A Berghof Speedwave MWS-3 model microwave digestion system was used for acid digestion of samples. In the roasting experiments, a laboratory tunnel furnace (Carbolite) was used.

**Table 1** Operating conditions for digestion by microwave oven.

	1	2	3	4
T ( $^\circ\text{C}$ )	100	160	180	100
Ta (min) <sup>a</sup>	10	10	10	10
Time (min) <sup>b</sup>	5	3	3	3

Note: <sup>a</sup> waiting time at desired temperature; <sup>b</sup> the time between the two sequential temperatures.

**Table 2** Operating conditions for ICP-OES.

Parameter	
Power (W)	1,450
Plasma gas flow rate (L·min <sup>-1</sup> )	15
Auxiliary gas flow rate (L·min <sup>-1</sup> )	0.2
Nebulizer gas flow rate (L·min <sup>-1</sup> )	0.8
Sample flow rate (L·min <sup>-1</sup> )	1.5
View mode	Axial-radial
Read	Peak area
Source equilibration time (s)	15
Read delay (s)	60
Replicates	3
Background correction	2-point (manual point correction)
Spray chamber	Scott type spray chamber
Nebulizer	Concentric Glass (Meinhard) Type A
Detector	Liquid state detector
Purge gas	Nitrogen
Shear gas	Air
Gas	Argon

**Table 3** The spectral wavelength of metal for ICP-OES.

Metal	Analytical wavelength (nm)
Cu	327.393
Co	228.616
S	181.975
Se	196.026
Te	214.281
Sb	206.836
As	193.696

### 3. Results and Discussion

The effects of roasting time, slag/pyrite/rate of copper concentrate and roasting temperature on the dissolution extents of metals were investigated in the leaching experiments.

Firstly, 220 g mixture of slag/pyrite which is 0.63% of Cu and 0.27% of Co was subjected to roasting at high temperatures in a closed medium for 2 hours and then 10 g samples were finally processed roasting air atmosphere at 600 °C at different times. Fig. 1 shows the effect of roasting time on metal dissolutions about 700 °C in a closed medium for 2 hours and then 10 g samples were finally processed roasting air atmosphere at 600 °C at different times and 1:1 slag/pyrite ratio. Under these conditions, 82.25% of Cu and 76.30% of Co were dissolved. Increasing

roasting time to 6 h increased Cu dissolution to 82%. In all cases, roasting temperature of 600 °C at 6 h was chosen to be the optimum condition.

220 g mixture of slag/pyrite/copper concentrate which is 5.25% of Cu and 0.22% of Co was subjected to roasting at high temperatures in a closed medium for 2 hours and then 10 g samples were finally processed roasting air atmosphere at 600 °C at different times. Fig. 2 shows the effect of roasting time on metal dissolutions about 700 °C in a closed medium for 2 hours and then 10 g samples were finally processed roasting air atmosphere at 600 °C at different times and 5:6:4 slag/pyrite/copper concentrate ratio. Under these conditions, 89.28% of Cu and 80.25% of Co were passed into the solution at the end of 6 hours.

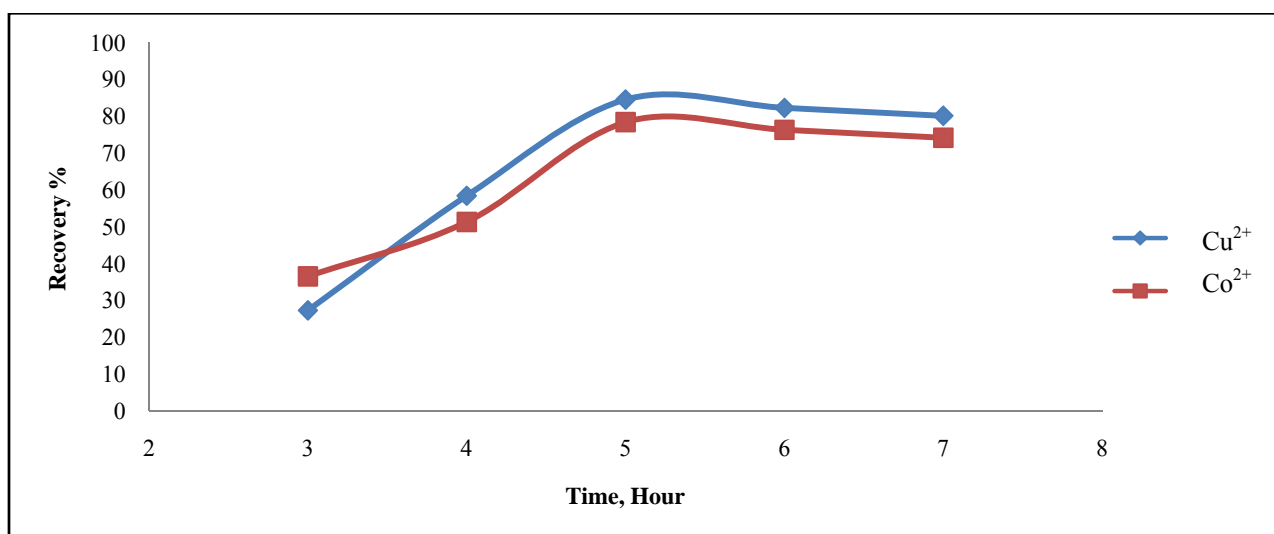


Fig. 1 Effect of roasting time on metal dissolutions at 600 °C and 1:1 slag/pyrite ratio.

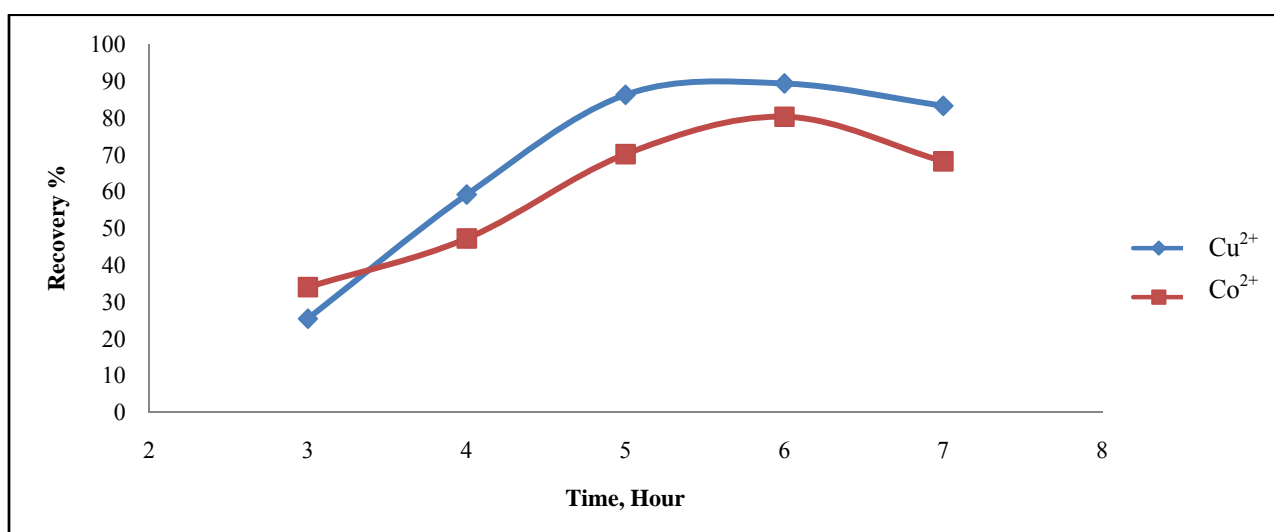


Fig. 2 Effect of roasting time on metal dissolutions at 600 °C and 5:6:4 slag/pyrite/copper concentrate ratio.

220 g mixture of slag/pyrite/copper concentrate which is 6.40% of Cu and 0.21% of Co was subjected to roasting at high temperatures in a closed medium for 2 hours and then 10 g samples were finally processed roasting air atmosphere at 600 °C at different times. Fig. 3 shows the effect of roasting time on metal dissolutions about 700 °C in a closed medium for 2 hours and then 10 g samples were finally processed roasting air atmosphere at 600 °C at different times and 4:6:5 slag/pyrite/copper concentrate ratio. Under these conditions, 93.10% of Cu and 85.60% of Co were passed into the solution at

the end of 5 hours.

After this, 220 g mixture of slag/pyrite/copper concentrate which is 8.10% of Cu and 0.20% of Co was subjected to roasting at high temperatures in a closed medium for 2 hours and then 10 g samples were finally processed roasting air atmosphere at 600 °C at different times. Fig. 4 shows the effect of roasting time on metal dissolutions about 700 °C in a closed medium for 2 hours and then 10 g samples were finally processed roasting air atmosphere at 600 °C at different times and 3:6:6 slag/pyrite/copper concentrate ratio. Under these conditions, 99.10% of

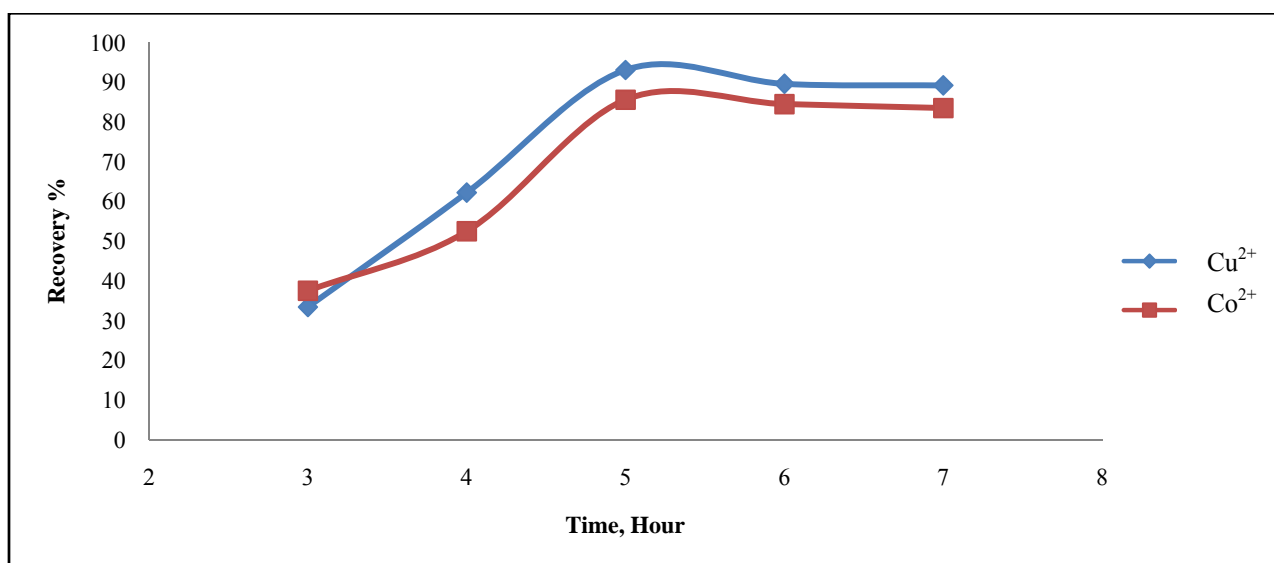


Fig. 3 Effect of roasting time on metal dissolutions at 600 °C and 4:6:5 slag/pyrite/copper concentrate ratio.

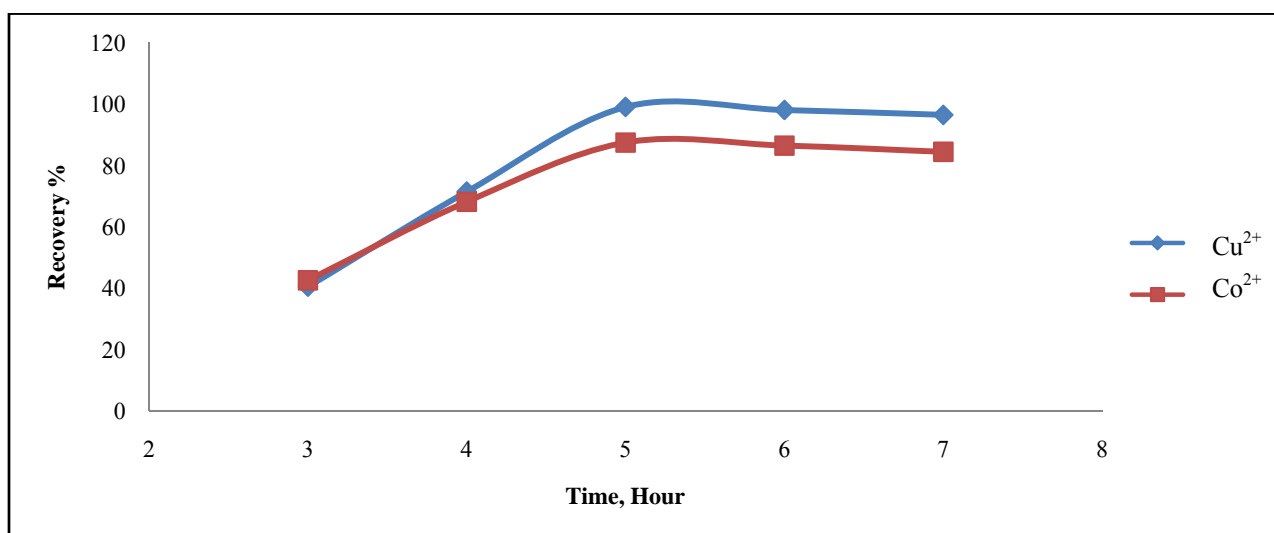


Fig. 4 Effect of roasting time on metal dissolutions at 600 °C and 3:6:6 slag/pyrite/copper concentrate ratio.

Cu and 87.50% of Co were passed into the solution at the end of 5 hours.

As seen in Figs. 1-4, effects of roasting times on the copper and cobalt values to the solution were observed. As shown in Table 4 and Fig. 5, as the rate of copper in mixture (slag/pyrite/copper concentrate ratio) increases, the copper and cobalt passed into the solution increases.

The mixtures (slag/pyrite/copper concentrate ratio: 3/6/6) were processed in a closed medium about 700 °C for two hours. Then, they were roasted at 600 °C for five hours. As seen in Figs. 1-4, roasting time was

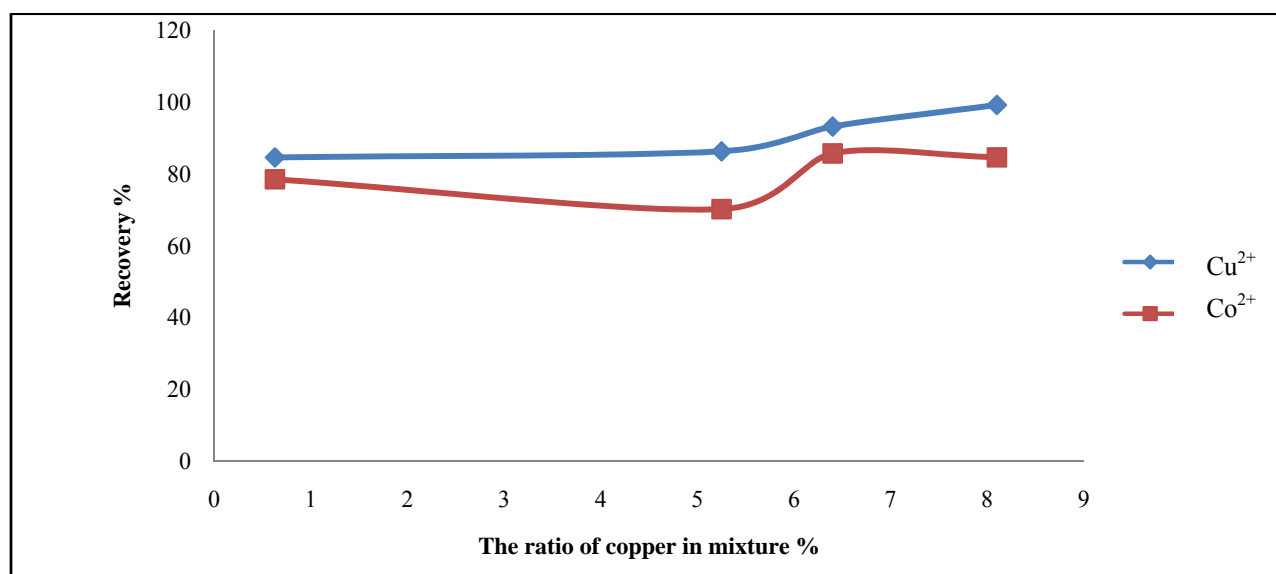
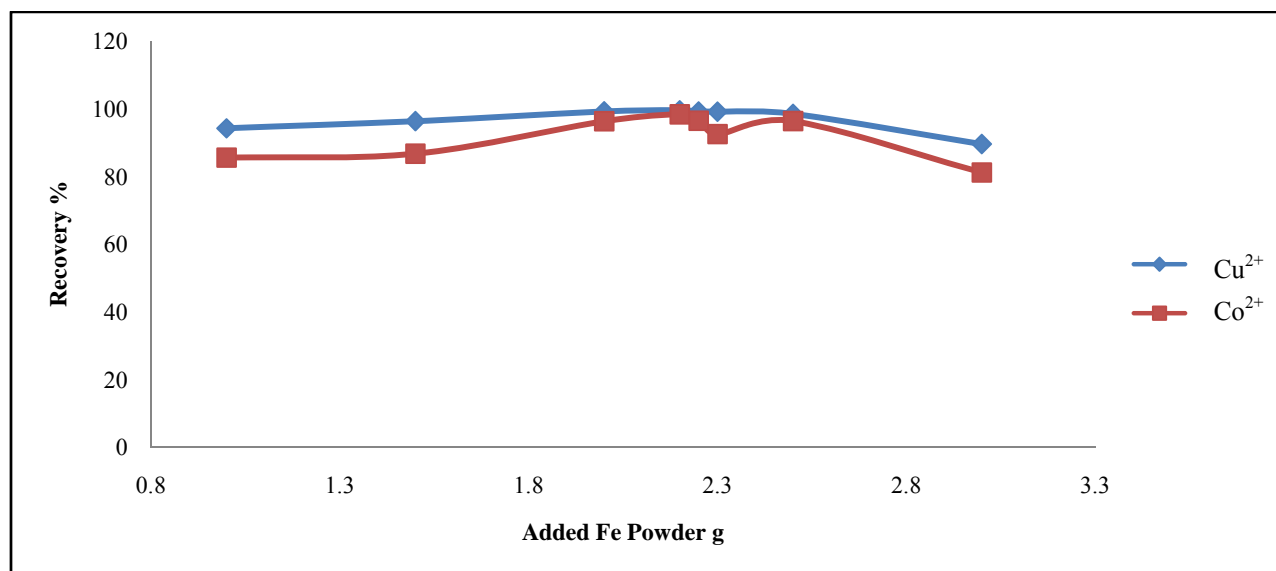
sufficient for five hours.

In the next experiments, after 1.00 g, 1.50 g, 2.00 g, 2.20 g, 2.25 g, 2.30 g, 2.50 g and 3.00 g of Fe powder was added to the mixtures (slag/pyrite/copper concentrate ratio: 3/6/6), 220 g of mixture (slag/pyrite/copper concentrate ratio: 3/6/6) were processed in closed medium about 700 °C and then the mixtures were roasted at 600 °C for 5 hours. The results are shown in Fig. 6.

As shown in Fig. 6, 2.20 g of Fe powder added to the mixtures (slag/pyrite/copper concentrate ratio: 3/6/6) is sufficient. Under these conditions, 99.60% of

**Table 4** Effect on the yield of the copper and cobalt of the rate of copper in the mixture (slag/pyrite/copper concentrate ratio) roasting air atmosphere at 600 °C for 5 hours.

Sample	The ratio of copper in mixture	Element	
		Cu%	Co%
slag/pyrite: 1/1	0.627	84.50	78.40
slag/pyrite/copper concentrate: 5/6/4	5.250	86.20	70.10
slag/pyrite/copper concentrate: 4/6/5	6.40	93.10	85.60
slag/pyrite/copper concentrate: 3/6/6	8.10	99.10	84.50

**Fig. 5** Effect on the yield of the copper and cobalt of the rate of copper in the mixture (slag/pyrite/copper concentrate ratio).**Fig. 6** Effect on the recovery of copper and cobalt of the iron powder added to the mixture.

Cu and 98.40% of Co passed into solution. Copper and cobalt separation from the solution was made on operation conditions [13]. In addition, entire of arsenic, antimony, selenium and telluride in the mixture was

removed from the structure in the result of work done in the closed system. After this, after roasting in the atmospheric environment, copper and cobalt could be taken to solution very high efficiency. Patent relating

to the study is detailed [14].

#### 4. Conclusions

For copper and cobalt recovery from copper slags, a binary mixture primarily formed by taking 1:1 pyrite/slag ratio. The mixture of slag/pyrite which is 0.63% of Cu and 0.27% of Co was subjected to roasting at high temperatures in a closed medium for 2 hours and then roasted at air atmosphere at 600 °C at different times. Under these conditions, 82.25% of Cu and 76.30% of Co were passed to the solution. After the creation of a ternary mixture, a mixture of 3:6:6 slag/pyrite/copper concentrate which is 8.10% of Cu and 0.20% of Co was subjected to roasting at high temperatures in a closed medium for 2 hours and then roasted in an air atmosphere at 600 °C under optimum temperature. Under these conditions, it is shown that 99.10% of Cu and 87.50% of Co were passed into the solution.

The effect of the yield of Cu and Co participating in the mixture of slag/pyrite/copper concentrate of iron powder was investigated. As seen from Table 4, 2.20 g Fe powder was added to 220 g of a mixture of 3:6:6 slag/pyrite/copper concentrate and 10 g of the mixture was roasted at 600 °C for 5 hours. It is shown that 99.60% of Cu and 98.40% of Co were passed into aqueous solution. Addition of Fe powder, the yields of copper and cobalt passing to the solution has increased remarkably. The addition of Fe powder to the mixture of copper and cobalt, spinel structure in the structure of the mixture has led to a deterioration in a closed medium and air atmosphere and has provided sulphation as a result of roasting. At the same time, Se, Te, As and Sb [14] completely removed the addition of iron powder to triple mixture in a closed medium.

#### References

- [1] Anand, S., Rao, K. S., and Jena, P. K. 1983. "Pressure Leaching of Copper Converter Slag Using Dilute Sulphuric Acid for the Extraction of Cobalt, Nickel and Copper Values." *Hydrometallurgy* 10 (3): 305-12.
- [2] Ziyadanogullari, R. 1992. "A New Method for Recovering Fe(II) Sulfate, Copper, and Cobalt from Converter Slag." *Separation Science and Technology* 27 (3): 389-98.
- [3] Ziyadanogullari, B. 2000. "Recovery of Copper and Cobalt from Concentrate and Converter Slag." *Separation Science and Technology* 35 (12): 1963-71.
- [4] Anand, S., Rao, P. K., and Jena, P. K. 1980. "Recovery of Metal Values from Copper Converter and Smelter Slags by Ferric Chloride Leaching." *Hydrometallurgy* 5 (4): 355-65.
- [5] Sukla, L. B., Panda, S. C., and Jena, P. K. 1986. "Recovery of Cobalt, Nickel and Copper from Converter Slag through Roasting with Ammonium Sulphate and Sulphuric Acid." *Hydrometallurgy* 16 (2): 153-65.
- [6] Altundogan, H. S., and Tumen, F. 1997. "Metal Recovery from Copper Converter Slag by Roasting with Ferric Sulphate." *Hydrometallurgy* 44 (1-2): 261-7.
- [7] Anand, S., Das, R. P., and Jena, P. K. 1981. "Reduction-roasting and Ferric Chloride Leaching of Copper Converter Slag for Extracting Copper, Nickel and Cobalt Values." *Hydrometallurgy* 7 (3): 243-52.
- [8] Bese, A. V. 2007. "Effect of Ultrasound on the Dissolution of Copper from Copper Converter Slag by Acid Leaching." *Ultrasonics Sonochemistry* 14 (6): 790-6.
- [9] Zhang, Y., Man, R., Ni, W., and Wang, H. 2010. "Selective Leaching of Base Metals from Copper Smelter Slag." *Hydrometallurgy* 103 (1): 25-9.
- [10] Arslan, C., and Arslan, F. 2002. "Recovery of Copper, Cobalt and Zinc from Copper Smelter and Converter Slags." *Hydrometallurgy* 67 (1): 1-7.
- [11] Ziyadanogullari, B., and Ziyadanogullari, R. 1999. "The Recovery of Copper and Cobalt from Oxidized Copper Ore and Converter Slag." *Turk. J. Chem.* 23 (1): 51-6.
- [12] Arslan, C. 1982. "Evaluation of Black Sea Copper Works' Smelter Slags via Acid Roasting Method." MS thesis, Istanbul Technical University.
- [13] Aydin, F., and Ziyadanogullari, R. 2007. "Separation of Copper, Cobalt and Iron in Solution Obtained from Copper Ore." *Asian Journal of Chemistry* 19 (7): 5537.
- [14] Ziyadanogullari, R., Tegin, I., and Guzel, R. 2009. A new technological application of beneficiation of copper ore (direct production from selenium and tellurium, removal of antimony and arsenic, gold and silver production from the rest left after copper and cobalt production). Turkey Patent TR 2009 10112 B, filed December 31, 2009, and issued October 10, 2012.

# Evaluation of Pb, Cu, Zn and Cd Levels in Some Plants at Roadsides between Mafraq and Jerash, Jordan

Abdullah Trad Al-fawwaz<sup>1</sup> and Khaled Abdu Al-Khazaleh<sup>2</sup>

1. Department of Biological Sciences, Al al-Bayt University, Mafraq 25113, Jordan

2. Department of Physics, Al al-Bayt University, Mafraq 25113, Jordan

**Abstract:** In this study, Cu, Zn, Cd and Pb concentrations were investigated in both stem and roots of three different plants which are Charlock (*Sinapis arvensis*), Inula (*Inula salicina*) and Asphodelus (*Asphodelus fistulosus*). The plants were collected from the roadsides between Mafraq and Jerash in Jordan. The concentrations were in  $\mu\text{g}$  of heavy metal per gram of sample weight. While the average concentrations in plants stem were  $0.16 \mu\text{g/g}$ ,  $9.5 \mu\text{g/g}$ ,  $0.51 \mu\text{g/g}$  and  $22.9 \mu\text{g/g}$  for Cd, Cu, Pb and Zn ions, respectively, the corresponding concentrations in the plants roots were  $0.09 \mu\text{g/g}$ ,  $6.4 \mu\text{g/g}$ ,  $0.2 \mu\text{g/g}$  and  $15.7 \mu\text{g/g}$  for the same ions. The measured concentrations were much less than those reported by other local and international studies, therefore, the area under investigation might be considered healthy for crops culturing.

**Key words:** Heavy metals, roadside plants, pollution.

## 1. Introduction

Plants are the primary sources of food for both humans and animals. Animals, on the other hand, serve as an essential food source for the human beings. For an efficient and healthy growth of plants, there must be soil, water and air, which jointly make up the favorable environments for the plants. Therefore, the purity of these favorable conditions is critical for the prevalence of healthy food. However, there are certain metal ions, which may enter the plants' cell cytosol, thus preventing them from activating the catalytically active proteins or structural proteins, which could otherwise protect them from the possible poisoning by heavy metals [1].

Vehicular emissions are considered primary sources of heavy metals that pollute the environment. Over the past three decades, the number of vehicles rapidly increased, resulting in a corresponding increase in environmental pollutants from vehicle emissions. Higher concentration of heavy metals in the

environment is quite hazardous to both animals and plants' health due to their toxicity. These extreme levels are thereby extremely dangerous to humans, plants and animals. The increment of traffic volume ultimately increases the accretions of such heavy metals. Vehicles emit a lot of toxic metals, which accumulate or build up along the roadside environments [2]. Consequently, heavy-metal pollution resulting from the increased traffic emissions may significantly contaminate the roadside crops, as well as plants that grow near the major highways [3].

Some of the metals that are essential constituents of certain alloys, wires, pipes and vehicle tires include Cu, Zn and Cd. These metals may be released to the surrounding environments near the highways as a result of mechanical corruptions and breakdowns [4]. For instance, lead (Pb) metal deposits along the roadside soils may accumulate in the form of lead sulfate [5]. As well, Cd metal emissions are primarily from consumption of oil lubricants and vehicle tire corruptions. Zinc metal pollution comes from the car-tire corruptions and the galvanized car parts, such as fuel tanks [6]. Furthermore, the most common source of Pb and Cu emissions is the vehicle braking

---

**Corresponding author:** Abdullah Trad Al-fawwaz, Ph.D., main research fields: microbial biotechnology, environmental control and algal ecology.



## 2.2 Sample Preparation Procedure

The sample preparation took place in the Analytical Chemistry Section at JAEC (Jordan Atomic Energy Commission). The samples were prepared according to SOP3 (Standard Operation Procedure 3) for sample preparations as:

(1) The samples were dried overnight at a temperature of 105 °C and the moisture was calculated;

(2)  $0.25 \pm 0.0001$  g of the dried samples was accurately measured and taken from every sample;

(3) After that, 1.3 mL HF (Hydrofluoric Acid), 8 mL HNO<sub>3</sub> and 2 mL H<sub>2</sub>O<sub>2</sub> (Hydrogen Peroxide (30%)) solutions were added to the accurately measured samples;

(4) Using Milestone ETHOS1, the samples were then digested through the microwave digestion system;

(5) The digested samples were then volumetrically transferred into 50 mL centrifuge test-tubes under room temperature and pressure;

(6) At the next step, the transferred samples were treated with 4% boric acid. This acid was used to remove any residue or excesses HF;

(7) Subsequently, NF 1200 centrifuge system was utilized for the classification of samples, after which the samples were diluted to 50 mL. This step was the very last step in the prime chemical preparations;

(8) Once again, the samples were diluted with 1% sub-boiled nitric acid (HNO<sub>3</sub>, 65%). This process was repeated twice (double dilution factor), hence the last dilution volume was 100 mL, for ICP-MS (Inductively Coupled Plasma-Mass Spectrometry) measurements;

(9) Finally, the Analytical Technique Measurement was employed, where the ICP-MS was used to determine the concentration of the elements. Six calibration standards from Accuracy Reference Standards were then prepared for all the items of interest. As well, a blank was prepared in 1%

sub-boiled nitric acid (65%). The internal standards utilized were Y, Tb and In. Furthermore, Bruker 810/820-Mass Spectrometer was used for sample measurements in order to establish the concentration of (Cu, Cd, Zn and Pb) elements.

## 3. Results and Discussion

Zn, Pb, Cu and Cd concentrations were measured in three types of plants on the upper part of their stems and leaves, and in roots from four different sites along the roadway. The measured concentrations were compared in Figs. 2 and 3.

Fig. 2 shows the concentration levels of heavy metals—Zn, Pb, Cu and Cd in the stem of Charlock, Inula and Asphodelus in the sites 1, 2, 3 and 4. From Fig. 2, it can be seen that Cd level is almost the least in all plants. On the other hand, Zn concentration level is always the highest, followed by Cu concentration level.

Fig. 3 reveals the levels of the concentration of heavy metals in the roots of the sampled plants. Cd and Cu concentrations are always below those of Pb and Zn. Besides, Zn concentration was always the highest in each test.

All the concentration levels of the heavy metals in all types of the studied plants and sites are shown in Tables 1a and 1b. It can be seen that the concentration levels of the four heavy metals in the stem of the plants are always greater than those found in the plant's roots at all sites. This indicates that the contamination from the surface environments is much more than that of the underground. No industrial pollutants exist in the neighboring areas in which the roadways exit. Thus, the vehicle emission could be the most conventional source for the pollution.

As seen in Table 2, the concentrations of the four heavy metals in the sampled plants are displayed. It shows the mean concentration levels of the heavy metals—Zn, Pb, Cu and Cd in the stems of the plant samples at the four sampled sites.

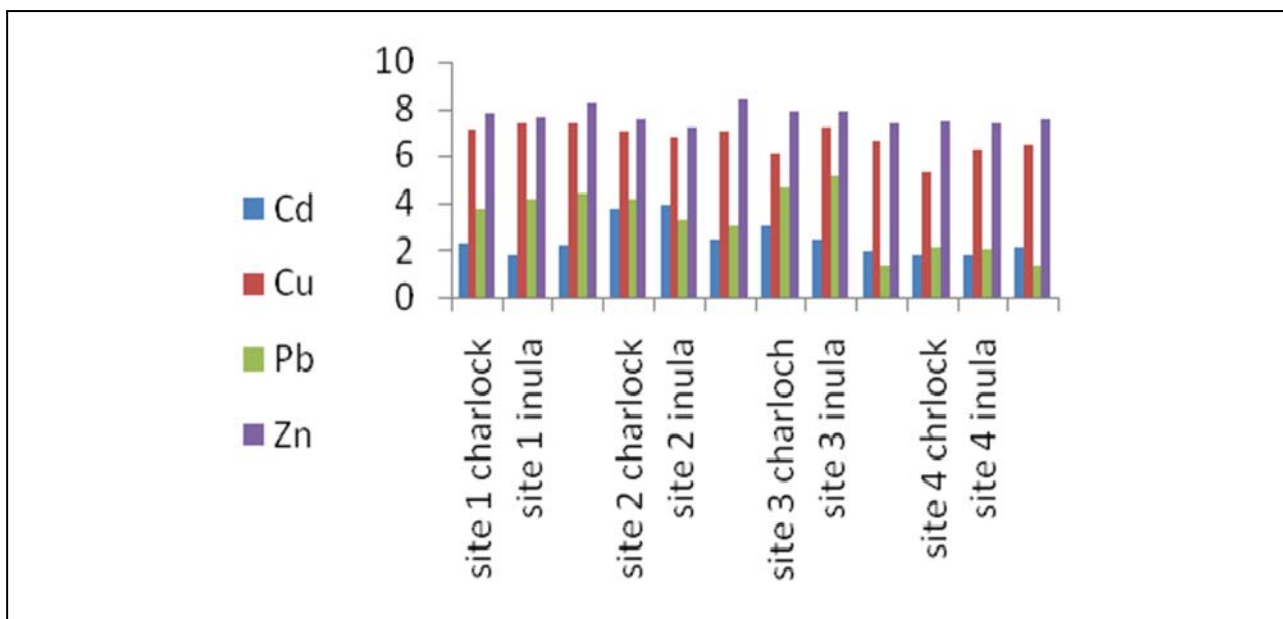


Fig. 2 The concentration of heavy metals—Zn, Pb, Cu and Cd in the stem of the Charlock (*Sinapis arvensis*), Inula (*Inula salicina*) and Asphodelus (*Asphodelus fistulosus*) in the four sites.

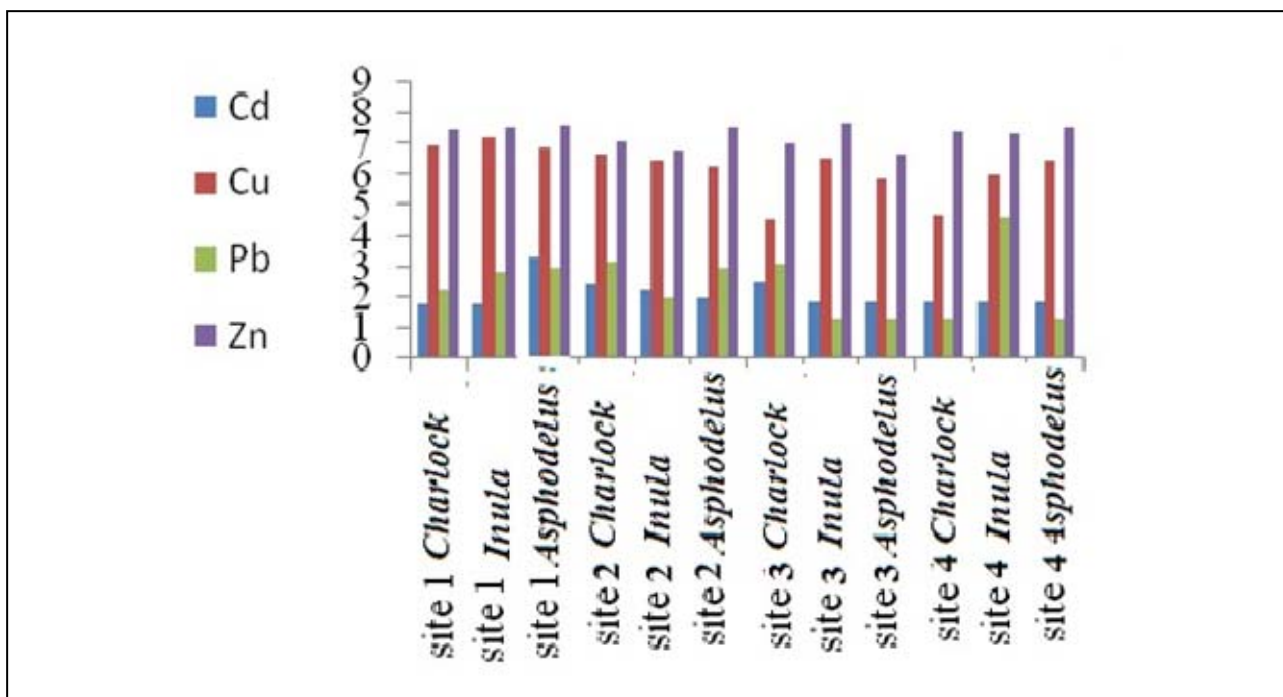


Fig. 3 The concentration of heavy metals—Zn, Pb, Cu and Cd in the roots of the Charlock (*Sinapis arvensis*), Inula (*Inula salicina*) and Asphodelus (*Asphodelus fistulosus*) at the four sites.

**Table 1a** The concentrations (in  $\mu\text{g/g}$ ) of Zn, Pb, Cu and Cd in the S (Stems) of Charlock (*Sinapis arvensis*), Inula (*Inula salicina*) and Asphodelus (*Asphodelus fistulosus*) at four different sites along the Mafraq-Jerash roadway.

ID	Cd ( $\mu\text{g/g}$ )	Cu ( $\mu\text{g/g}$ )	Pb ( $\mu\text{g/g}$ )	Zn ( $\mu\text{g/g}$ )
Site 1/Charlock/S	$0.101 \pm 0.043$	$12.215 \pm 0.336$	$0.434 \pm 0.045$	$23.561 \pm 2.140$
Site 1/Inula/S	$< 0.064$	$16.573 \pm 1.916$	$0.631 \pm 0.081$	$19.764 \pm 1.879$
Site 1/Asphodelus/S	$0.092 \pm 0.254$	$15.359 \pm 1.134$	$0.827 \pm 0.105$	$37.268 \pm 3.914$
Site 2/Charlock/S	$0.427 \pm 0.036$	$11.549 \pm 1.170$	$0.617 \pm 0.051$	$18.091 \pm 1.725$
Site 2/Inula/S	$0.513 \pm 0.046$	$9.086 \pm 0.924$	$0.276 \pm 0.007$	$13.473 \pm 1.287$
Site 2/Asphodelus/S	$0.118 \pm 0.028$	$11.814 \pm 1.018$	$0.219 \pm 0.036$	$42.210 \pm 3.991$
Site 3/Charlock/S	$0.2190 \pm 0.069$	$4.584 \pm 0.417$	$1.072 \pm 0.089$	$27.361 \pm 2.511$
Site 3/Inula/S	$0.116 \pm 0.034$	$13.626 \pm 1.245$	$1.824 \pm 0.091$	$25.441 \pm 2.617$
Site 3/Asphodelus/S	$0.071 \pm 0.004$	$7.216 \pm 0.687$	$< 0.038$	$15.274 \pm 1.461$
Site 4/Charlock/S	$< 0.064$	$2.12 \pm 0.249$	$0.081 \pm 0.004$	$17.251 \pm 1.607$
Site 4/Inula/S	$< 0.064$	$5.276 \pm 0.507$	$0.075 \pm 0.006$	$16.384 \pm 1.482$
Site 4/Asphodelus/S	$0.084 \pm 0.005$	$5.281 \pm 0.447$	$< 0.038$	$18.637 \pm 1.758$

**Table 1b** The concentrations (in  $\mu\text{g/g}$ ) of Zn, Pb, Cu and Cd in the R (Root) of Charlock (*Sinapis arvensis*), Inula (*Inula salicina*) and Asphodelus (*Asphodelus fistulosus*) at four different sites along the Mafraq-Jerash roadway.

ID	Cd ( $\mu\text{g/g}$ )	Cu ( $\mu\text{g/g}$ )	Pb ( $\mu\text{g/g}$ )	Zn ( $\mu\text{g/g}$ )
Site 1/Charlock/R	$< 0.064$	$10.194 \pm 1.291$	$0.094 \pm 0.062$	$17.543 \pm 1.583$
Site 1/Inula/R	$< 0.064$	$13.914 \pm 1.516$	$0.172 \pm 0.138$	$19.079 \pm 2.051$
Site 1/Asphodelus/R	$0.281 \pm 0.356$	$9.571 \pm 0.618$	$0.194 \pm 0.028$	$20.115 \pm 2.351$
Site 2/Charlock/R	$0.117 \pm 0.008$	$8.251 \pm 0.907$	$0.247 \pm 0.031$	$11.861 \pm 1.064$
Site 2/Inula/R	$0.097 \pm 0.008$	$6.729 \pm 0.593$	$0.073 \pm 0.003$	$9.358 \pm 1.005$
Site 2/Asphodelus/R	$0.074 \pm 0.032$	$5.316 \pm 0.421$	$0.199 \pm 0.033$	$19.348 \pm 2.018$
Site 3/Charlock/R	$0.121 \pm 0.034$	$0.993 \pm 0.116$	$0.224 \pm 0.062$	$11.057 \pm 1.271$
Site 3/Inula/R	$< 0.064$	$6.927 \pm 0.713$	$< 0.038$	$21.109 \pm 2.221$
Site 3/Asphodelus/R	$< 0.064$	$3.618 \pm 0.401$	$< 0.038$	$8.094 \pm 0.811$
Site 4/Charlock/R	$< 0.064$	$1.090 \pm 0.094$	$< 0.038$	$16.215 \pm 1.514$
Site 4/Inula/R	$< 0.064$	$4.214 \pm 0.381$	$1.024 \pm 0.103$	$15.940 \pm 1.391$
Site 4/Asphodelus/R	$< 0.064$	$6.417 \pm 0.571$	$< 0.038$	$18.523 \pm 1.902$

**Table 2** The concentrations of the four heavy metals ( $\mu\text{g/g}$ ) in the sampled plants' stems from all the sites.

ID	Cd ( $\mu\text{g/g}$ )	Cu ( $\mu\text{g/g}$ )	Pb ( $\mu\text{g/g}$ )	Zn ( $\mu\text{g/g}$ )
Site 1	0.084333	14.71567	0.630667	26.86433
Site 2	0.352667	10.81633	0.370667	24.59133
Site 3	0.135333	8.475333	0.978	22.692
Site 4	0.07	3.97	0.06	17.42

Table 2 further shows that there is no significant difference in the contaminations between the first three sites and the least contaminations observed at site 4. This outcome may be due to the kind of land terrain, where site 4 happened to be an open mountainous area. From the study, authors can assert that the heavy metal pollutants from the air eventually

precipitate and accumulate on the ground surface. However, depending on the wind flow and patterns, the precipitated concentrations on the adjacent areas either increased or decreased [5]. The analysis can thereby conclude that the wind carries the vehicle emissions away from the roadsides; hence the fewer contaminations observed.

**Table 3** The concentration of the four heavy metals ( $\mu\text{g/g}$ ) in the sampled plants' roots from all the sites.

ID	Cd $\mu\text{g/g}$	Cu $\mu\text{g/g}$	Pb $\mu\text{g/g}$	Zn $\mu\text{g/g}$
Site 1	0.133667	11.22633	0.153333	18.91233
Site 2	0.096	6.765333	0.173	13.52233
Site 3	0.083	3.846	0.1	13.42
Site 4	0.06	3.91	0.37	16.89

A similar scenario could be noticed in Table 3, which shows the heavy metal concentrations in the sampled plants' roots. As displayed in Table 3, some levels in the roots of the sampled plants in site 4 are higher than those found on the remaining sites. The reason for this result is that the nature of mountainous soils allows parts of the plants' roots to grow above the ground, thereby exposing them to the air pollutants. On the other hand, the remaining sites are plain/open areas with agricultural soils that cover the roots underground, thus preventing them from the exposure to the air pollutants.

The average concentration levels in the stems of the plant samples in this study are  $22.9 \mu\text{g/g}$ ,  $0.51 \mu\text{g/g}$  and  $9.5 \mu\text{g/g}$  for Zn, Pb and Cu, respectively. These concentration levels are much less than those found in the plant samples at the roadside of the road connecting Amman to the southern part of Jordan, which were found to be  $98.7 \mu\text{g/g}$ ,  $7.3 \mu\text{g/g}$  and  $31.3 \mu\text{g/g}$  for Zn, Pb and Cu, respectively [12]. As well, the levels were less than those of the roadway between Ramtha and Mafraq, which were  $41.5 \mu\text{g/g}$ ,  $0.6 \mu\text{g/g}$ ,  $9.2 \mu\text{g/g}$  and  $0.3 \mu\text{g/g}$  for Zn, Pb, Cu and Cd, respectively [13]. Howari, F. M., et al. [14] found that the concentration levels for Cd, Pb and Zn along the roadsides between north Shuna and Aqaba through Dead Sea high way were  $5 \mu\text{g/g}$ ,  $79 \mu\text{g/g}$  and  $79 \mu\text{g/g}$ , respectively.

It can be seen that the contamination levels of the investigated heavy metals along the roadsides between Mafraq and Jerash are much less than those found on the other studied roadways in Jordan. This scenario could be explained by two major reasons: firstly, the traffic volume could be less than that in other studies

roadways; secondly, the humid climate for the studied areas, especially, the sites 2, 3, and 4, were most likely to be less contaminated than site 1. Authors' results are also less than those along the north Shuna and Aqaba. This outcome could be related to the open and mountainous areas of authors' study. The roadway from Shuna to Aqaba is below the sea level and is mostly neighbored by mountains to the eastern sides. The occurrence of these mountains could form a barrier that decreases the wind speed and increases the accumulation of emissions on the nearby roadsides.

Internationally, Alshammari, A. M. [15] found that the levels of Zn, Pb, Cu and Cd along the urban roadsides of Hail in Saudi Arabia are  $197 \mu\text{g/g}$ ,  $89 \mu\text{g/g}$ ,  $53 \mu\text{g/g}$  and  $5 \mu\text{g/g}$ , respectively. In Nepal, the corresponding concentrations at roadside farmlands were  $62.57 \mu\text{g/g}$ ,  $5.57 \mu\text{g/g}$ ,  $25.89 \mu\text{g/g}$  and  $0.34 \mu\text{g/g}$ , respectively [2]. In a study conducted to establish the concentration of these metals in the neighboring Çorlu-Çerkezköy highway in Turkey, the levels were  $20 \mu\text{g/g}$ ,  $1 \mu\text{g/g}$  and  $8.2 \mu\text{g/g}$  for Zn, Pb and Cu, respectively [16]. Along Bangalore city railway station in India, the concentrations were  $60.3 \mu\text{g/g}$ ,  $64.3 \mu\text{g/g}$ ,  $36.6 \mu\text{g/g}$  and  $7.5 \mu\text{g/g}$  for Zn, Pb, Cu and Cd, respectively [17]. Christiana, C. M. O. and Samuel, K. [18] found the concentration of these metals to be  $0.06 \mu\text{g/g}$ ,  $0.07 \mu\text{g/g}$ ,  $0.15 \mu\text{g/g}$  and  $0.13 \mu\text{g/g}$ , respectively, along the roadway in Adogo in Nigeria.

Authors' results are comparable to some of the international results. As such, it can be seen that the highest concentration levels were in Hail in Saudi Arabia, which can support authors' suggestion that the dry climate could be a reasonable influence on the

increased contamination levels caused by vehicle emissions. The concentration levels were also high along the northern Jordan highway, which also has a dry climate. Also, the type of the used fuel is another important reason for the contamination levels observed above.

#### 4. Conclusions

In this study, concentration levels for all the investigated heavy metals—Zn, Pb, Cu and Cd were almost within the acceptable limits in plants. These levels were less than those in other areas in Jordan, and also less than those found in the other international studies. Comparing authors' results with others, in and outside Jordan, it can be concluded that dry weather supports the contamination with heavy metals that come from the vehicle emissions. On the other hand, the open humid roadsides could be less contaminated as compared to the other closed humid roadsides. Finally, utilizing these areas as agricultural land could produce low contaminated crops with fewer health hazards.

#### Acknowledgements

The authors express their gratitude to JAEC for their unlimited cooperation and to Al al-Bayt University for using facilities in the Department of Biological Sciences and their technical and financial assistance.

#### References

- [1] Zenk, M. H. 1996. "Heavy Metal Detoxification in Higher Plants—A Review." *Gene* 179 (1): 21-30.
- [2] Yan, X., Zhang, F., Zeng, C., Zhang, M., Devkota, L. P., and Yao, T. 2012. "Relationship between Heavy Metal Concentrations in Soils and Grasses of Roadside Farmland in Nepal." *Int. J. Environ. Res. Public Health* 9 (9): 3209-26.
- [3] Zeng, H. 2008. "Advance in the Study on Effects of Traffic and Transportation on Soil and Plants on Both Sides of the Road." *J. Meteorol. Environ.* 24: 52-5.
- [4] Jaradat, Q. M., Masadeh, A., Zaitoun, M. A., and Maitah, B. M. 2005. "Heavy Metal Contamination of Soil, Plant and Air of Scrapyard of Discarded Vehicles at Zarqa City, Jordan." *Soil & Sediment Contam.* 14 (5): 449-62.
- [5] Harrison, R. M., Laxen, D., and Wilson, S. J. 1981. "Isolation and Characterization of Heavy Metal Resistant Microbes." *Environ. Sci. Technol.* 15: 1379-83.
- [6] Falahi-Ardakani, A. 1984. "Contamination of Environment with Heavy Metals Emitted from Automobiles." *Ecotoxicol. Environ. Saf.* 8 (2): 152-61.
- [7] Winther, M., and Slentø, E. 2010. *Heavy Metal Emissions for Danish Road Transport*. National Environmental Research Institute, Aarhus University.
- [8] U.S. Government. 2001. "Control of Emissions of Hazardous Air Pollutants from Mobile Sources: Final Rule." *Fed. Regis.* 66: 80-6.
- [9] Sinha, S., Pandey, K., Gupta, A. K., and Bhatt, K. 2005. "Accumulation of Metals in Vegetables and Crops Grown in the Area Irrigated with River Water." *Bul. Environ. Contam. Toxicol.* 74 (1): 210-8.
- [10] Wuana, R. A., and Okieimen, F. E. 2011. "Heavy Metals in Contaminated Soils: A Review of Sources, Chemistry, Risks and Best Available Strategies for Remediation." *Isrn Ecology* 2011. doi:10.5402/2011/402647.
- [11] Willers, S., Gerhardsson, L., and Lundh, T. 2005. "Environmental Tobacco Smoke (ETS) Exposure in Children with Asthma—Relation between Lead and Cadmium, and Cotinine Concentrations in Urine." *Respir. Med.* 99 (12): 1521-7.
- [12] Jaradat, Q. M., and Momani, K. A. 1999. "Contamination of Roadside Soil, Plants and Air with Heavy Metals in Jordan, a Comparative Study." *Turk. J. Chem.* 23 (2): 209-20.
- [13] Al-Khazaleh, K. A. 2016. "The Concentration of Cd, Cu, Pb and Zn Heavy Metals in Plants along the Highway between Ramtha and Mafraq." *JNSR* 6 (22): 44-9.
- [14] Howari, F. M., Abu-Rukah, Y., and Goodell, P. C. 2004. "Heavy Metal Pollution of Soils along North Shuna-Aqaba Highway, Jordan." *IJEP* 22 (5): 597-607.
- [15] Alshammari, A. M. 2011. "Seasonal Variations of Soil Heavy Metal Contaminants along Urban Roads: A Case Study from the City of Hail, Saudi Arabia." *JJCE* 5 (4): 581-91.
- [16] Ekmekyapar, F., Sabudak, T., and Seren, G. 2012. "Assessment of Heavy Metal Contamination in Soil and Wheat (*Triticum aestivum* L.) Plant around the Corlu-Cerkezkoy Highway in Thrace Region." *Global Nest Journal* 14 (4): 496-504.
- [17] Deepalakshmi, A. P., Ramakrishnaiah, H., Ramachandra, Y. L., and Kumar, N. N. 2014. "Leaves of Higher Plants as Indicators of Heavy Metal Pollution along the Urban Roadways." *IJST* 3 (6): 304-6.
- [18] Christiana, C. M. O., and Samuel, K. 2013. "Investigation of Heavy Metal Levels in Roadside Agricultural Soil and Plant Samples in Adogo, Nigeria." *Acad. J. Environ. Sci.* 1 (2): 31-5.

# Eco-friendly Leather: Chromium Reduction in the Tanning Cycle

Elena Salernitano<sup>1</sup>, Alessandra Strafella<sup>1</sup>, Mercedes Roig<sup>2</sup> and Alice Dall'Ara<sup>1</sup>

1. Laboratory of TEMAF (Materials Technologies Faenza), Italian National Agency for New Technologies, Energy and Sustainable Economic Development (ENEA), Faenza 48018, Italy

2. INESCOP, Centre for Technology and Innovation, Elda 03600, Spain

**Abstract:** The leather manufacturing is traditionally responsible for high environmental pollution. Tannery effluent contains, indeed, large amounts of lime sludge, sulfides, acids, toxic metals salts, in particular chromium salts, which are toxic, non-biodegradable and hardly disposable. For this reason, great research efforts are addressed to establish a significantly eco-sustainable and convenient business for companies and to produce high quality leather products. The replacement of current commercial chemical and toxic products with innovative natural/naturalized products and technologies in some crucial phases of the tanning cycle (mainly bating and defatting), can induce an eco-friendly reduction of the needed chromium amount. Leather samples, treated with innovative bating and defatting products and tanned by several different Cr contents, were characterized by SEM-EDS (Scanning Electron Microscopy equipped with Energy Dispersive X-Ray Spectroscopy) and TGA (Thermogravimetric Analysis). SEM-EDS was used to observe the surface and cross-section morphology and to provide a semi-quantitative elemental analysis, while TGA to evaluate the thermal stability and decomposition phases. The compatibility of the innovative products was demonstrated and the environmental impact of the process, performed by the effluents characterization, was effectively improved as a result of a 20% Cr lowering. The use of innovative products and the chromium reduction did not affect the thermal stability, leather morphology and not involve significant differences in the composition.

**Key words:** Leather manufacturing, tanning cycle, Cr reduction, natural/naturalized products.

## 1. Introduction

Leather production via hides and skins processing is a way to enhance recovery of agro-industrial by-products (circular economy). On the other hand, these processes are very demanding on resources and energy (environment). One ton of bovine salted raw hides produce up to 250 kg of finite leather, requiring about 40 m<sup>3</sup> of water and 400-500 kg of reagents, often chemicals [1]. The leather manufacturing provides a negative image of itself mainly because of the environmental impact of tannery wastes [2]. Conventional leather processing methods, indeed, significantly contribute to the pollution. The wastewaters contain non-biodegradable hazardous chemicals (especially chromium), the solid wastes are

hardly disposable and volatile organic compounds are emitted to the atmosphere.

The leather processing involves many phases that modify the physical, chemical and biological properties of the raw skin/hide. The main five phases of the whole tanning cycle are: bating, defatting, tanning, fatliquoring and dyeing. Bating and defatting are part of the preparatory stage that includes all the operations carried out to prepare the hide/skin for tanning. The tanning phase converts them into a stable, dried and flexible material no longer subject to putrefaction; the most common tanning method is based on the use of chromium salts. The post-tanning operations include fatliquoring and dyeing.

The current main environmental, social and economic goals of leather industry are to reduce the environmental impact and/or to develop a chromium-free tanning cycle [3, 4].

---

**Corresponding author:** Elena Salernitano, Ph.D., research field: materials development and characterization.

In this work, leather samples processed by bating, defatting and tanning, defined as wet blue, were prepared using different chromium percentages with the purpose to demonstrate that the replacement of the current commercial bating and defatting agents with natural/naturalized products allows a 20% reduction of Cr salts, maintaining the leather high quality standards and workability.

The activities were carried out in the framework of LIFE14 ENV/IT/443 LIFETAN (eco-friendly tanning cycle) project. The overall aim of the project is to substitute some reagents (toxic or from nonrenewable sources) with natural products or from renewable sources. Traditional/standard reagents for bating and degreasing phases were substituted by innovative products:

- bating agent obtained from poultry manure treated according to a European patent [5], and demonstrated in the framework of LIFE10 ENV/IT/365PODEBA (use of poultry dejection for the bating phase in the tanning cycle) project [6-8];
- degreasing agent obtained from lactose via chemical synthesis [9].

## 2. Material and Methods

The commercial and natural/naturalized bating and defatting agents were compared and their influence in the tanning process was examined. Laboratory tests were carried out in rotating stainless steel tanning drums, measuring 300 mm in diameter and 150 mm in width respectively, featuring systems for automation, control and dosage of water and reactants (Fig. 1).

Several tests have been performed with four different chromium salts concentrations: 4%, 5%, 6% and 8% over pelt weight (w/w) with natural/naturalized products. They were compared with standard process (standard bating and degreasing agent and 8% concentration of Cr salts).

In each test with cattle hides, 3 sq. foot pieces of pelt hides with a thickness of 1.8-2.0 mm were processed. These pieces of wet blue cattle hides had



**Fig. 1** Laboratory-scale tanning drums.

been prepared for the tanning operation by means of a standard process of soaking, liming and unhairing. After the tanning process, the wet blue leathers were dried and the shrinkage temperature was determined.

Once every stage was completed, a sample of the residual bath and a sample of each one of the obtained wet blue leathers were taken for their characterization. The environmental evaluation was performed by the characterization of the effluents in accordance with international standards. The selected wastewater control parameters and the related standards are: pH (ISO 10523:2008), TKN (Total Kjeldahl Nitrogen), COD (Chemical Oxygen Demand) (ISO 6060:1989), BOD<sub>5</sub> (Biochemical Oxygen Demand after 5 days) (ISO 5815-1:2003) and biodegradability (determined as BOD/COD).

The four wet blue leather samples, tanned with different chromium concentration (4% w, 5% w, 6% w and 8% w), were characterized by SEM-EDS (Scanning Electron Microscopy equipped with Energy Dispersive X-Ray Spectroscopy) and TGA (Thermogravimetric Analysis).

The SEM characterization was used to observe the surface and cross-section morphology of leather samples [3, 10, 11], while the EDS semi-quantitative analysis was performed to provide the leather elemental composition. A LEO 438 VP, equipped with EDS microanalysis Oxford Link ISIS 300 was used. The analysis was performed in variable pressure and back scattered electrons were detected. These conditions allow the samples observation with no need

of pretreatment, avoiding any damages or contaminations. Moreover, the leather samples were enough dry to be directly observed without specific drying treatment. In all samples, the surface and cross-section observation and the semi-quantitative analysis were carried out on different areas to obtain more representative and reliable results.

TGA was performed to evaluate the thermal stability and decomposition phases [10]. A STA 409 simultaneous analyzer (Netzsch, Selb, Germany) equipped with TGA sample carrier supporting an S type thermocouple was used. The samples weight loss was measured (TGA expressed as % weight loss). The first derivative of the TGA (inflection point I.P.) trace represents the weight loss rate DTG (Derivative Thermogravimetric Analysis) (expressed as  $\% \cdot \text{min}^{-1}$ ) and is used for the exact identification of the relative decomposition steps. The analyses were performed on about 150 mg of material, placed in a sample carrier of 3.4 mL in volume, under dynamic inert Ar atmosphere with a flow rate of 100 mL/min and a heating rate of 10 °C/min up to 1,400 °C. The Netzsch TA window software was used for the results data processing.

### 3. Results and Discussion

The environmental evaluation of the process was performed by the characterization of the residual baths both from the bating/defatting stages and the tanning stage, as reported in Table 1.

The residual baths from the innovative bating/defatting stages exhibited a lower conductivity than those from commercial bating/defatting stages. The COD and BOD<sub>5</sub> of effluents from the bating/defatting stage and the tanning stage are higher.

These results can be ascribed to both the chemical composition of the defatting product that is a derivate of lactose, and the improved defatting action of naturalized products. Biodegradability is greatly improved by natural products. TKN is reduced by naturalized products in bating stage, the phases with the higher N load in tanning cycle. Regarding the chromium content of the residual bath, a greater fixation of the chromium to the collagen is observed by using naturalized bating and defatting products, which is observed in the lower chromium content of the residual tanning bath; 620 mg/L versus 740 mg/L, that means a reduction of around 15%. This indication will be the object of future tests at pre-industrial scale. This is an indication of good performance of new products, thus suggesting to investigate the possibility to carry out the tanning processes with lower Cr contents.

Wet blue samples obtained with 4%, 5%, 6% and 8% were characterized. The eco-friendly wet blue leathers showed good physical strength and adequate smoothness, softness, fullness and flexibility.

After drying, the shrinkage temperature was determined in order to verify if the naturalized bating agent can make a better maceration in the cross-section, increasing the diffusion and the transport of the tanning agent within the pelts and, consequently, allow a reduction of chromium concentration maintaining the same leather quality.

The results are reported in Table 2, showing that with the use of the naturalized bating agent, the chromium salts concentration can be effectively reduced in order to achieve a shrinkage temperature of 100 °C, which is considered suitable for the manufacture of footwear and other leather articles.

**Table 1** Characterization of residual baths.

	Bating/defatting agents	pH	COD (mg/L)	BOD <sub>5</sub> (mg/L)	Biodegradability	TKN (mg/L)	Chromium (mg/L)
Effluents from bating/defatting	commercial/commercial	8.64	7,300	1,387	0.19	1,650	---
	naturalized/natural	8.15	14,800	5,290	0.36	880	---
Effluents from 8% Cr tanning	commercial/commercial	5.09	7,700	3,120	0.41	---	740
	naturalized/natural	5.25	11,500	5,260	0.46	---	620

**Table 2 Chromium percentage vs shrinkage temperature of wet blue leather samples.**

Chromium (weight %)	Shrinkage T (°C)
4	93
5	97
6	99
8	103

Regarding to the COD and BOD, these trials show higher values due to the higher defatting effect and the chemical composition of the ecodefating products which is a derivate of lactose, but in this case, the biodegradability of the residual baths is a 70% higher employing the natural innovative defatting agent, as described in LIFE13 ENV/IT/470ECODEFATTING (environmentally friendly natural products instead of chemical products in the degreasing phase of the tanning cycle) project.

About the nitrogen content in the bating/defatting residual baths, the lower values have been got employing the deodorized Laying Hen Manure (PODEBA) and this reduction is higher by using in combination with the ecodefating natural product.

The morphological wet blue leather surface characterization by SEM revealed a homogeneous pores distribution with uniform size (Fig. 2). Some residual salt crystals, mainly in 5% and 4% chromium tanned leather, were observable. These last two leathers showed also deeper pores.

A representative spectrum of the average surface semi-quantitative composition for every sample is provided in Fig. 3. The main result of EDS microanalysis was the reduction of chromium content congruently with the percentage of chromium salts used in the tanning phase.

The EDS confirmed the presence of some surface salt crystals, mainly in the case of the 5% chromium tanned leather; the microanalysis restricted to a surface residue highlighted a high content of sodium and chlorine, while the microanalysis restricted to the substrate showed oxygen and carbon as the main elements.

The morphological cross-section characterization highlighted a more compact layer on the sample top

and a more fibrous aspect on the bottom (Fig. 4). The top compact layer was thicker in the 8% and 6% chromium tanned leather than in the 5% and 4% samples; the 4% chromium tanned leathers exhibited a lower thickness. In contrast to the surface, the residues of salt crystals were negligible in the cross-section of all observed wet blue leathers. The cross-section of all observed leathers showed satisfactory opening up extent of fibers, suggesting that post tanning chemicals could easily penetrate into the fibers network.

The EDS microanalysis pointed out, also in the cross-section composition, the reduction of chromium content congruently with the percentage of chromium used in the leather tanning process.

The reduction of Cr content, both in the surface and in the cross-section of Cr-tanned leathers, depending

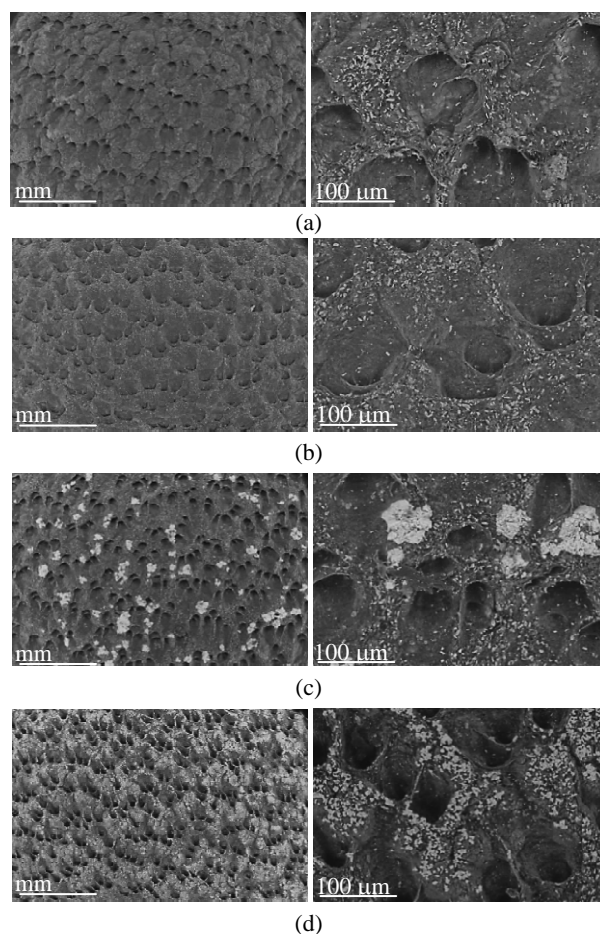


**Fig. 2 Surface micrographs at different magnifications of 8 (a), 6 (b), 5 (c) and 4 (d) %Cr tanned wet blue leathers.**

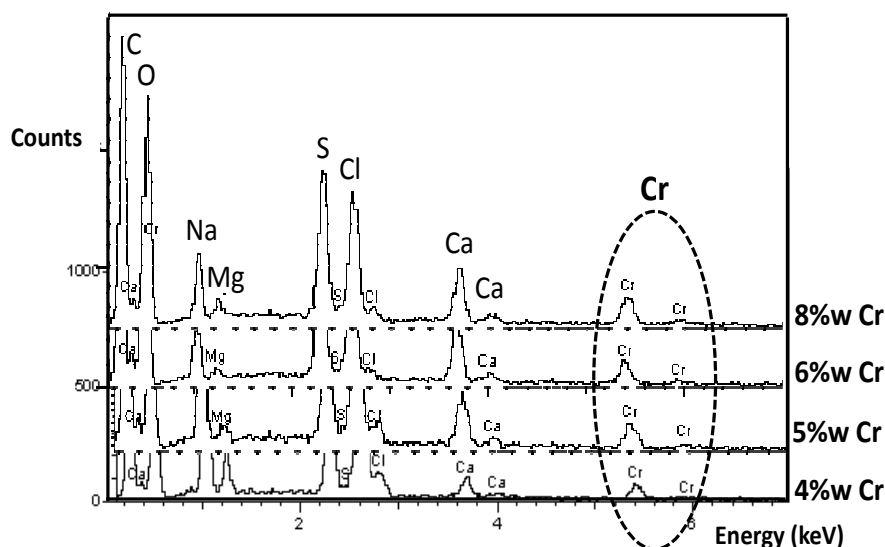


Fig. 3 Typical surface EDS spectrum of wet blue leathers.

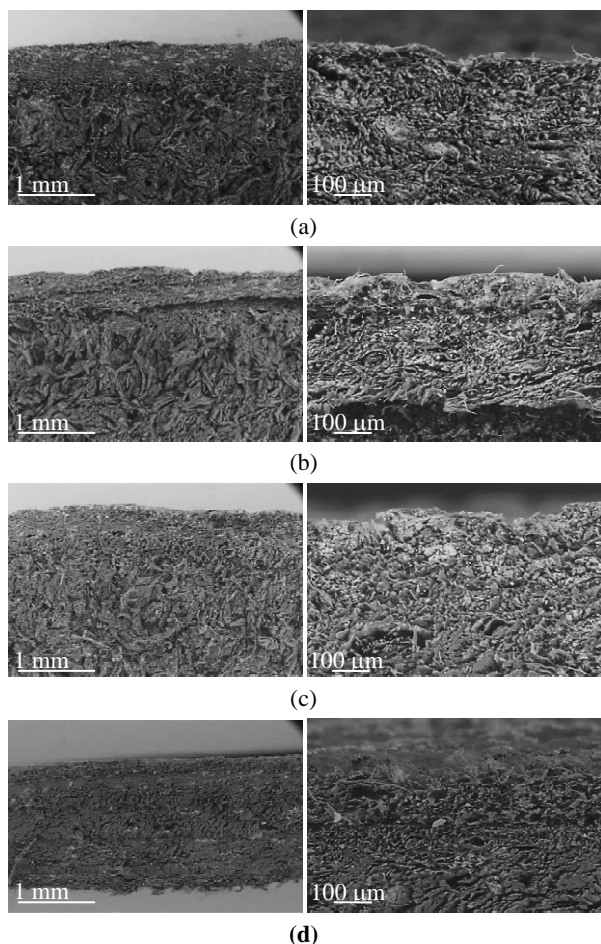


Fig. 4 Cross-section micrographs at different magnifications of 8 (a), 6 (b), 5 (c) and 4 (d) %Cr tanned wet blue leather.

on the amount of Cr used in tanning phase is shown in Fig. 5. A higher Cr content in the leather cross-section than in the surface was revealed in all observed wet-blue samples. The 5% and 6% chromium tanned leathers showed a very similar Cr content, both on the surface and in the cross-section.

The TGA detected similar thermograms for all samples, with four mass loss steps, as confirmed by DTG curve (Fig. 6): 1st step 25-225 °C; 2nd step 225-550 °C; 3rd step 550-850 °C; 4th step 850-1,400 °C.

The first stage of the mass loss is due to the evaporation of the adsorbed or not-structured water which has a maximum degradation rate at around 100 °C; the thermal stability is the same for all samples, except the water percentage. The main step (200-550 °C) corresponds to the decomposition of organic matter and pyrolysis of aliphatic compounds; it was ascribable to the thermal decomposition of collagen. The collagen and elastin constitute the dermis and are the main components of the leather; they are structural proteins made of polypeptide chains whose primary blocks are the amino acids. The collagen structure explains the higher intensity and wider shape of the second DTG peak and the great

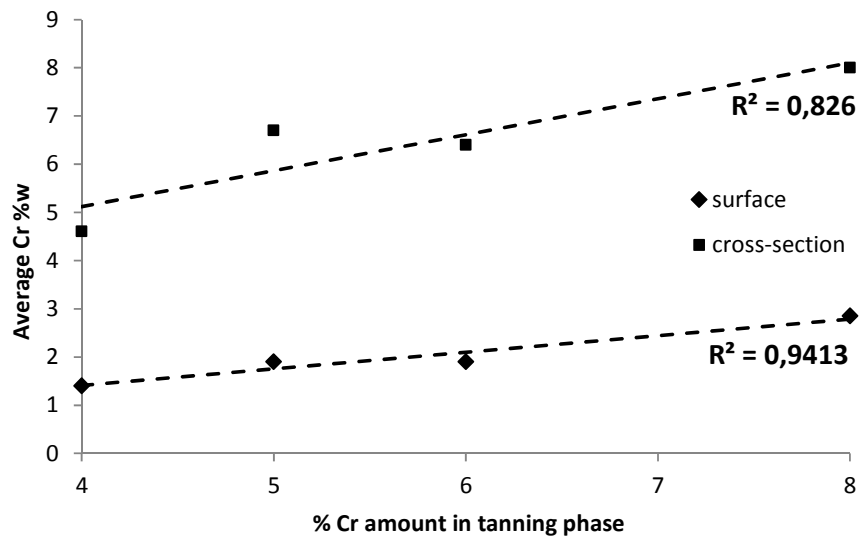


Fig. 5 Comparison between surface and cross-section average Cr content in wet blue leathers.

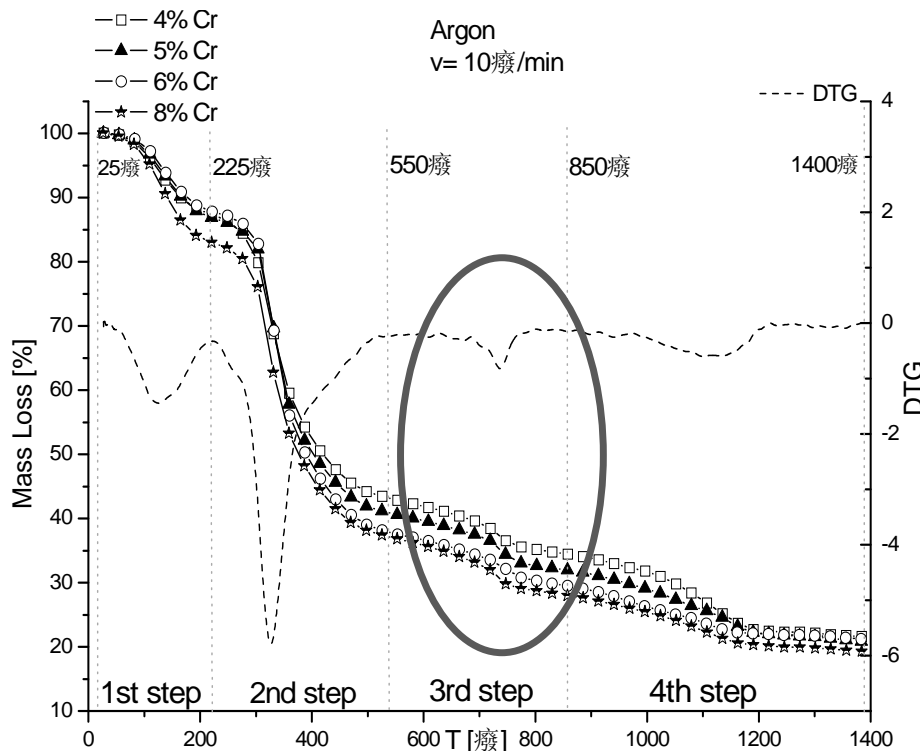


Fig. 6 TGA and typical DTG in argon of Cr tanned wet blue leathers.

mass loss at 200-550 °C. At this evolution temperature range, the decomposition of many products takes place [12]:

- The formation of ammonia from the amino and imino groups of the amino acids of leather occurs at around 300 °C under gradual heating in the thermobalance. The collagen-based materials contain

about 8-13% nitrogen and the formation of significant amount of ammonia, in lines with the expectations;

- At about 300 °C, the scission of the hydroxyl groups (structured water) and the development of CO<sub>2</sub> and SO<sub>2</sub> take place;
- At about 350 °C, it is noticed the presence of molecular ion of acetonitrile and ion of pyrrole. The

main amino acid constituents of collagen are glycine, proline, alanine and hydroxyproline. Pyrrole can be formed from the pyrrolidine rings of proline and hydroxyproline;

- The release of aliphatic alkenyl and alkyl compounds occurs at higher temperatures, in the range 400-550 °C;
- The formation of other molecular compounds occurs: toluene (at about 450 °C), ascribable to the scission of the side groups of phenylalanine, CO<sub>2</sub> and SO<sub>2</sub>, from 300 °C [12].

All these reactions justify the DTG shape between 200 °C and 550 °C, resulting from the overlapping of different decomposition rate peaks. The collagen degradation increases with chromium percentage.

The third mass loss step (550-850 °C) is due to the decomposition of chromium compounds. All analyzed wet blue leathers exhibited a similar mass loss value, thus showing the same thermal stability not affected by the chromium percentage. Therefore, the use of natural/naturalized products in the bating and defatting phases can effectively allow a reduction of chromium amount in the tanning phase.

Moreover, the temperature corresponding to the third DTG peak was about 750 °C and it is also due to the minerals degradation, such as the decomposition of calcium carbonate.

The last step (850-1,400 °C) is attributable to inorganic fraction decomposition; their decomposition occurs around 900-1,000 °C.

During the second mass loss stage, CO<sub>2</sub> is produced and the crosslinked network structure of a macromolecular chain favors the char forming reactions under thermal decomposition in inert atmosphere. Then, the kinetic of the reaction between CO<sub>2</sub> and char was significantly favored at high temperatures, having an exponential dependence on temperature:



It can be assumed that the last peaks of DTG, at about 1,000 °C, were due to this reaction [13].

## 5. Conclusions

A set of wet blue leather samples was analyzed to evaluate the effectiveness of the chromium amount reduction in the tanning phase, even reducing the environmental impact of the process, consequently to the replacement of standard products with innovative natural/naturalized products in the bating and defatting phases. The eco-friendly wet blue leathers showed good physical strength and adequate smoothness, softness, fullness and flexibility.

According to these results, authors can conclude that PODEBA bating agent improves the chrome tanning process and it is possible to use lower concentration of chromium salts (20% less) to obtain the same quality of final leather, measured by means the shrinkage temperature determination.

The most significant considerations to be derived from the SEM-EDS analysis are:

- Both the reduction of chromium content in the tanning phase and the replacement of standard chemical products in the bating and defatting phases, did not significantly affect the leather morphology;
- All the wet-blue leathers showed homogeneous pores surface distribution with uniform size;
- A certain amount of salt crystals residues were clearly visible on the surface of samples;
- The cross-section of all observed leathers showed satisfactory opening up extent of fibres, suggesting that post tanning chemicals could easily penetrate into the fibres network;
- The cross-section was characterized by a two layer structure with a more compact layer on the sample top (thicker in the leathers tanned with higher Chromium amount) and a more fibrous aspect on the bottom;
- The microanalysis pointed out a reduction of chromium content, congruently with the percentage of chromium used in the tanning process, both in the surface and cross-section composition;
- The Cr content was higher in the leather cross-section than in the surface in all observed

samples of the first set (the 5% and 6% Cr tanned leathers showed a very similar Cr content, both on the surface and in the section).

TGA in argon revealed four mass loss steps: evaporation of the adsorbed or not-structured water, decomposition of collagen, chromium compounds and inorganic fraction. All wet blue leather samples exhibited the same thermal stability whatever the chromium percentage is.

## Acknowledgment

These experimental results were obtained within the framework of the project LIFE 14 ENV/IT/443LIFETAN (eco-friendly tanning cycle), co-financed by EU, within the LIFE programme.

## References

- [1] Black, M., Canova, M., Rydin, S., Scalet, B. M., Roudier, S., and Sancho, L. D. 2013. "Best Available Techniques (BAT) Reference Document for the Tanning of Hides and Skins." *European Commission Database*. Accessed August 23, 2017. [http://eippcb.jrc.ec.europa.eu/reference/BREF/TAN\\_Published\\_def.pdf](http://eippcb.jrc.ec.europa.eu/reference/BREF/TAN_Published_def.pdf).
- [2] Dixit, S., Yadav, A., Dwivedi, P. D., and Das, M. 2015. "Toxic Hazards of Leather Industry and Technologies to Combat Threat: A Review." *Journal of Cleaner Production* 87: 39-49.
- [3] Wang, Y. N., Zeng, Y., Zhou, J., Zhang, W., Liao, X., and Shi, B. 2016. "An Integrated Cleaner Beamhouse Process for Minimization of Nitrogen Pollution in Leather Manufacture." *Journal of Cleaner Production* 112: 2-8.
- [4] Saravanabhavan, S., Raghava Rao, J., Unni Nair, B., and Ramasami, T. 2007. "An Eco-efficient Rationalized Leather Process." *Journal of Chemical Technology and Biotechnology* 82 (11): 971-84.
- [5] Ridolfi, A., and Memmi, M. 2012. A process of maturing and stabilizing biomasses under reduction of smelling emissions. European Patent Specification EP Patent 1314710, filed November 26, 2001, and issued January 11, 2012.
- [6] <http://www.podeba.eu>. Accessed August 23, 2017.
- [7] Dall'Ara, A., Billi, L., La Peruta, M. T., Cepparone, A., and Roig, M. 2013. "PODEBA: An Industrial Symbiosis Case Extended Abstract." *Environmental Engineering and Management Journal* 12 (S11): 269-72.
- [8] Roig, M., Segarra, V., Martinez, M. A., and Ferrer J. 2013. "Environmental Alternatives to Bating and Fatliquoring Processes (Alternativas ambientales a los procesos de rendido y engrase)." *Technical Bulletin AQEIC Key Book (Boletín Técnico AQEIC Libro Clave)* 64: 91-101.
- [9] <http://www.life-ecodefating.com/en/>. Accessed August 23, 2017.
- [10] Fathima, N. N., Kumar, M. P., Rao, J. R., and Nair, B. U. 2010. "A DSC Investigation on the Changes in Pore Structure of Skin during Leather Processing." *Thermochimica Acta* 501 (1): 98-102.
- [11] Uehara, K., Toyoda, H., Chonan, Y., and Okamura, H. 1987. "Observation of Skins, Hides and Leathers with Scanning Electron Microscope. IV. Changes in Pig Skins during Bating Process." *The Journal of the American Leather Chemists Association (USA)* 82: 33-40.
- [12] Sebestyen, Z., Czegeny, Z., Badea, E., Carsote, C., Sendrea, C., Barta-Rajnai, E., et al. 2015. "Thermal Characterization of New, Artificially Aged and Historical Leather and Parchment." *Journal of Analytical and Applied Pyrolysis* 115: 419-27.
- [13] Tang, Y., Ma, X., Lai, Z., and Fan, Y. 2015. "Thermogravimetric Analyses of Co-combustion of Plastic, Rubber, Leather in N<sub>2</sub>/O<sub>2</sub> and CO<sub>2</sub>/O<sub>2</sub> Atmospheres." *Energy* 90: 1066-74.

# Fluorescence Properties of the Lanthanide Supported onto Titanate Nanosheets

Daisuke Yoshioka<sup>1</sup>, Yasumitsu Nishimura<sup>2</sup> and Ken-ichi Katsumata<sup>3</sup>

1. Department of Natural Sciences, Kawasaki Medical School, Kurashiki 701-0192, Japan

2. Department of Hygiene, Kawasaki Medical School, Kurashiki 701-0192, Japan

3. Photocatalysis International Research Center, Tokyo University of Science, Noda 278-8510, Japan

**Abstract:** Metal oxide nanosheets are increasingly used as catalysts, hard coatings and transparent thin films. Among these materials, TNSs (Titanate Nanosheets) synthesized in liquid phase enjoy particular attention due to their water dispersibility, photocatalytic activity, unique morphology and ease of synthesis. Importantly, the photo-induced redox reaction between TNSs and metal oxides affords potentially fluorescent metal-supported TNSs with enhanced photocatalytic activity, e.g., Ln/TNSs (Lanthanide-supported TNSs). Herein, TNSs doped with arbitrary amounts of group 5 elements (M-TNSs: M = V, Nb and Ta) were prepared to investigate the fluorescent excitation spectra of Ln/M-TNSs and thus shed light on the mechanism of photodeposition and determine the origin of Ln/TNS fluorescence. As a result, photodeposition was shown to involve phot-induced redox reaction between TNSs and lanthanide oxides, and the fluorescence intensity of Ln/TNSs and Ln/M-TNSs was demonstrated to be determined by the overlap of TNS and Ln<sup>3+</sup> excitation energies.

**Key words:** Photodeposition, photoluminescence, lanthanide, TNSs (Titanate Nanosheets), group 5 elements.

## 1. Introduction

Low-dimensional structures such as nanotubes and nanosheets continue to attract increased research attention [1-4], as exemplified by the wide use of TNSs (Titanate Nanosheets) in a variety of engineering, chemical and optical applications. Single nanosheets comprise ultra-thin ( $10^{-10}$ - $10^{-8}$  m) monocrystals and can be stacked to form a layered structure. Importantly, both identical and different nanosheets can be easily stacked, which allows various molecules (such as dyes, metal cations and organic compounds) to be intercalated within the layers [5-8]. As an example, metal oxide nanosheets and their derivatives are extensively exploited in diverse applications as (photo) catalysts, hard coats and functional transparent thin films [9-11].

Recently, several groups have synthesized TNSs by

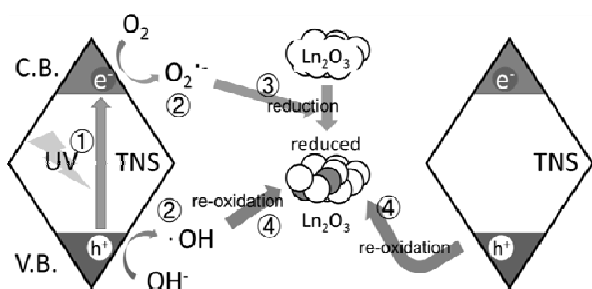
liquid-phase methods [1, 12], revealing that these materials exhibit diamond-like shape, water dispersibility and photocatalytic activity [13].

The photocatalytic activity of TNSs can be enhanced by decorating their surface with suitable metals to obtain metal/TNS composited. Unluckily, conventional photodeposition is not suited for this purpose, since the water dispersibility of liquid-phase-synthesized TNSs disturbs the separation of metal cation from the metal/TNS dispersion, requiring the use of metal oxides instead of metal salt solutions [14].

Herein, Ln/TNS (Lanthanide-supported TNS) were prepared by irradiating Ln oxides ( $\text{Sm}_2\text{O}_3$ ,  $\text{Eu}_2\text{O}_3$ ,  $\text{Tb}_2\text{O}_3$  or  $\text{Dy}_2\text{O}_3$ ) and TNS dispersions with UV (Ultraviolet) light (Scheme 1). Thus the synthesized Ln/TNS exhibited pronounced photoluminescence (particularly in the case of Eu/TNSs, which showed strong red fluorescence [14]) that was attributed to *f-f* transitions resulting from TNS excitation and energy transfer to Ln<sup>3+</sup>.

---

**Corresponding author:** Daisuke Yoshioka, Ph.D., main research fields: functional materials, low-dimensional materials and photocatalyst.



**Scheme 1** Mechanism of the photo-induced reaction between TNSs and  $\text{Ln}_2\text{O}_3$  resulting in Ln photodeposition: (1) Excitation of TNSs by UV irradiation; (2) generation of reactive oxygen species; (3) reduction of  $\text{Ln}_2\text{O}_3$  by superoxide anion radicals; and (4) re-oxidation to reduced  $\text{Ln}_2\text{O}_3$  by hydroxyl radicals and holes on the TNS surface.

Herein, TNSs doped with group 5 elements (M-TNSs: M = V, Nb and Ta) were synthesized to confirm the mechanism of the reaction occurring between TNSs and metal oxides during the photodeposition and clarify the origins of Ln/TNSs fluorescence and the TNS-to- $\text{Ln}^{3+}$  energy transfer. In view of the fact that Nb and Ta oxides exhibit photocatalytic activities similar to those of  $\text{TiO}_2$  and TNSs, whereas V oxides do not, Nb-TNSs and Ta-TNSs were expected to be photocatalytically active. If Nb-TNS and Ta-TNS behaved as the photocatalyst similar to TNS, Ln could be supported onto Nb-TNSs and Ta-TNSs, whereas V-TNS systems were predicted to exhibit decreased amounts of deposited Ln.

## 2. Experimental Section

### 2.1 Materials

Titanium tetraisopropoxide ( $\text{Ti}(\text{O}-i\text{Pr})_4$ ), 10 wt% aqueous solution of tetraethylammonium hydroxide ( $\text{NEt}_4\text{OH}$ ), 2-propanol, acetone and certain lanthanide oxides ( $\text{Sm}_2\text{O}_3$ ,  $\text{Eu}_2\text{O}_3$  and  $\text{Dy}_2\text{O}_3$ ) were purchased from Wako Pure Chemical Industries, Ltd. (Osaka, Japan) and used as received.  $\text{Tb}_2\text{O}_3$ , vanadium oxytriethoxide ( $\text{VO}(\text{OEt})_3$ ), niobium pentaethoxide ( $\text{Nb}(\text{OEt})_5$ ) and tantalum pentaethoxide ( $\text{Ta}(\text{OEt})_5$ ) were purchased from Sigma-Aldrich (St. Louis, MO, USA).

### 2.2 Apparatus Used for Synthesis

Hydrothermal treatment was performed in a 4749 general purpose acid digestion autoclave vessel (Parr Instrumental Company, Moline, IL, USA). A UVGL-25 (UVP, LLC, Upland, CA, USA) was used as a UV radiation source.

### 2.3 Apparatus Used for Instrumental Analysis

TEM (Transmission Electron Microscopy) imaging was performed using a JEM-1400 microscope (JEOL, Tokyo, Japan). TEM samples were prepared by drop casting dispersion onto a microgrid or a mesh grid (Cu). Fluorescence spectra of dispersions were obtained by using F-2700 instrument (Hitachi High-Tech Science Corporation, Tokyo, Japan).

### 2.4 TNS Synthesis

TNSs were synthesized from  $\text{Ti}(\text{O}-i\text{Pr})_4$  and  $\text{NEt}_4\text{OH}$  by the liquid-phase method [1, 12], and the as-prepared TNS dispersion was transferred to the autoclave and twice heated to 110 °C for 6 h in an oil bath.

An arbitrary volume of  $\text{Ti}(\text{O}-i\text{Pr})_4$  was mixed with  $\text{VO}(\text{OEt})_3$  in 2-propanol while keeping the total (Ti + V) concentration constant, followed by hydrolysis in the presence of  $\text{NEt}_4\text{OH}$  and hydrothermal treatment to obtain V-TNSs. Nb-TNSs and Ta-TNSs were obtained in a similar way.

To prepare Eu/TNSs, a suspension of  $\text{Eu}_2\text{O}_3$  powder in a TNS dispersion was UV-irradiated for 30 min, and unreacted  $\text{Eu}_2\text{O}_3$  was removed. Other Ln/TNSs were obtained in a similar way.

## 3. Results and Discussion

### 3.1 Effect of M Doping on TNS Structure

M-TNSs were synthesized from mixture of  $\text{Ti}(\text{O}-i\text{Pr})_4$  and corresponding alkoxide (see experimental section). The total metal (Ti + M) concentration in dispersion was held constant at 0.05 mol/L, and  $[\text{M}]/[\text{Ti} + \text{M}]$  ratio were adjusted to 0.1,

0.2, 0.33 and 0.5. As a result, the nanosheet size slightly decreased with increasing M loading (Fig. 1) and the diamond shape of nanosheets was slightly distorted at  $[M]/[Ti + M] = 0.5$ . Conversely, the thin sheet structure and water dispersibility of the obtained composites were preserved.

Thus, TNSs and M-TNS showed no remarkable structure or dispersibility differences, and M-TNSs were thus treated similarly to liquid-phase-synthesized TNSs.

### 3.2 $Ln^{3+}$ Supporting onto TNS and M-TNSs

$Ln/M$ -TNSs were synthesized by varying the lanthanide and the nature/loading of M. Fig. 2 shows the TEM images of  $Eu/M$ -TNSs, revealing that Ln deposition did not result in any morphological changes.

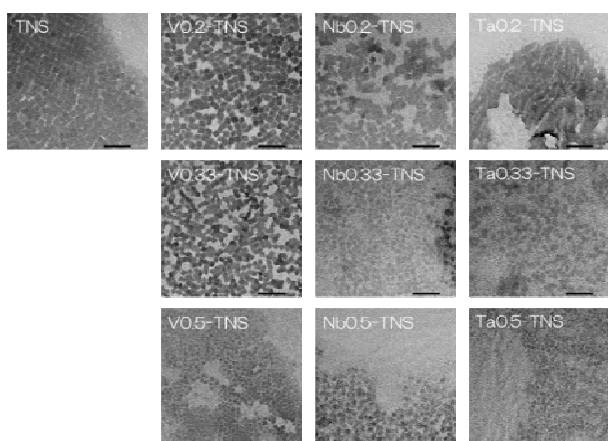


**Fig. 1** TEM images of TNSs and M-TNSs (Scale bars equal 100 nm).

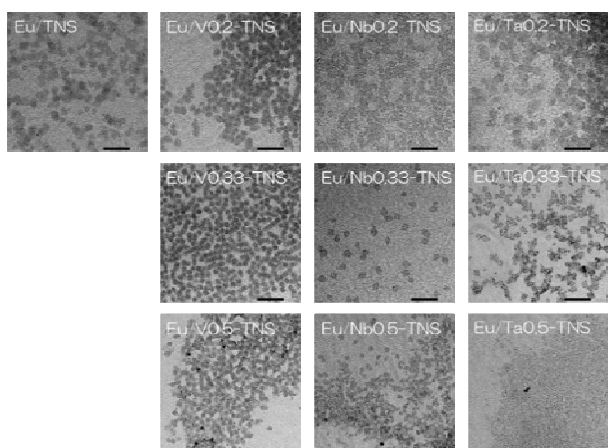


**Fig. 2** TEM images of  $Eu/TNS$  and  $Eu/M$ -TNSs (Scale bars equal 100 nm).

Dots observed on the diamond vertices for  $Eu/M0.5$ -TNS could correspond to clusters of  $Eu^{3+}$  (not identified), in which case these results would show that the amount of supported Ln species increased with increasing M loading.

Comparison of  $Ln/M$ -TNSs fluorescence excitation spectra provided interesting information on the mechanism of the deposition reaction and the origin of fluorescence (Fig. 3). Notably, the fluorescence intensity of  $Ln/V$ -TNSs decreased with increasing V content, and the corresponding fluorescence peak maxima shifted to longer wavelengths. Conversely, the fluorescence intensities of  $Ln/Nb$ -TNSs and  $Ln/Ta$ -TNSs mostly increased with increasing Nb or Ta contents, and the peak maxima shifted to red. Also, the supporting amount of Tb increased with increasing Nb or Ta loading, as confirmed by the increased fluorescence intensity of original  $Tb^{3+}$  peaks at 330-370 nm. The similar tendency was observed in  $Dy/Nb$ -system. In other systems, the TNS peaks at 300-310 nm were initially enhanced by the addition Nb or Ta, subsequently weakening at larger M loadings, with the blue shifts being similar to those observed for the above systems.

Since vanadium oxides do not exhibit photocatalytic activity, the incorporation of V into TNSs predictably decreased their activity, whereas the fluorescence intensities of  $Ln/Nb$ -TNSs and  $Ln/Ta$ -TNSs were mostly equal to those of original  $Ln/TNS$ s, suggesting that photodeposition involved a photo-induced redox reaction between TNSs and  $Ln_2O_3$ .

The TNS excitation peak at 300-310 nm was red-shifted by the addition of V, whereas a blue shift was observed for Nb or Ta addition, indicating a more pronounced  $M$ -TNS-to- $Ln^{3+}$  energy transfer in the latter case. The combination of this hypothesis with the Dieke diagram (Fig. 4) [15] allowed authors to explain the Ln-specific effects of M incorporation on the fluorescence spectra of  $Ln/M$ -TNSs.

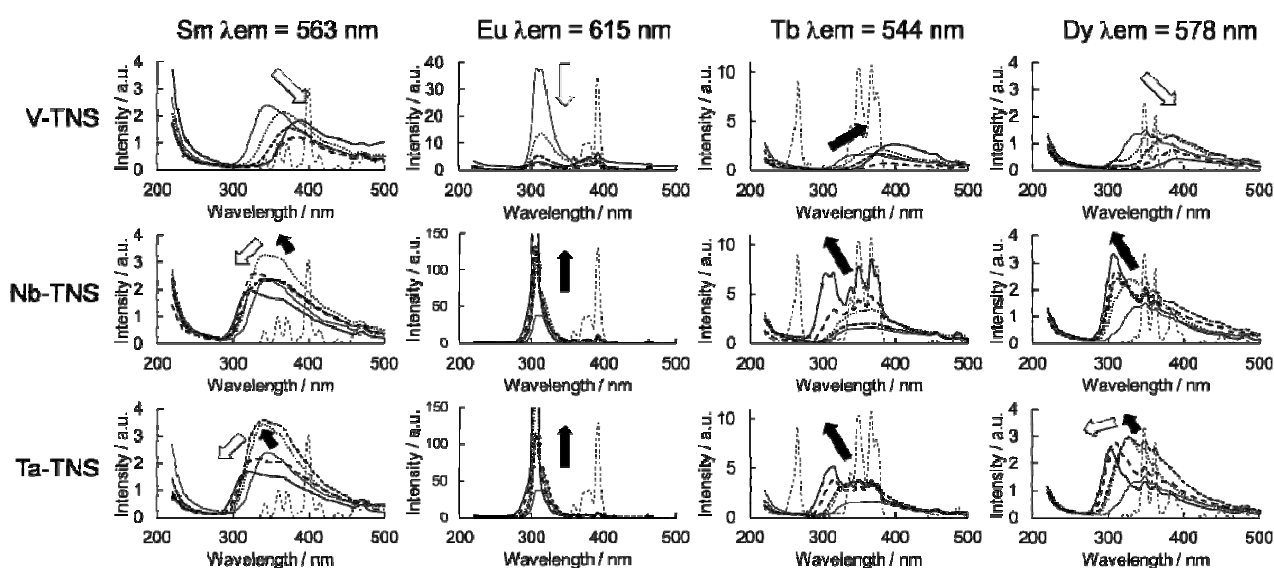


Fig. 3 Fluorescence excitation spectra of Ln/M-TNSs (Solid line: Ln/TNSs; dotted line: Ln/M0.1-TNSs; broken line: Ln/M0.2-TNSs; long broken line: Ln/M0.33-TNSs; bold solid line: Ln/M0.5-TNSs; and narrow broken line:  $\text{Ln}_2\text{O}_3$  dissolved in aqueous  $\text{HNO}_3$ ; Arrows shows the behaviors of peaks with increasing M loading).

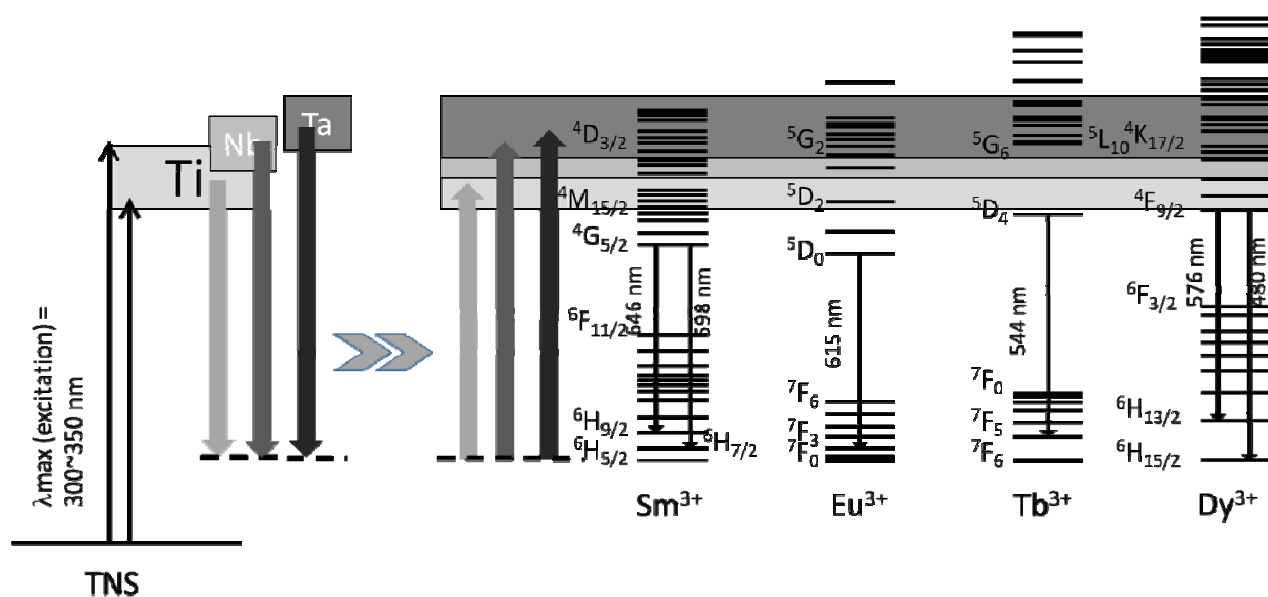


Fig. 4 Overlap between the excited energy levels of M-TNSs and those of  $\text{Ln}^{3+}$ , drawn according to the Dieke diagram.

Upon excitation with UV light, Nb-TNSs and Ta-TNSs received slightly more energy than original TNSs, transferring it to surface-deposited  $\text{Ln}^{3+}$  ions and thus inducing electronic transitions to higher levels than in the case of M-free Ln/TNSs. For  $\text{Eu}^{3+}$  and  $\text{Tb}^{3+}$ , radiationless deactivation did not occur until the lowest excitation level was reached due to the wide gap between excitation levels observed for these  $\text{Ln}^{3+}$ , resulting in increased probabilities (and hence,

intensities) of Ln/M-TNS emission. In the case of  $\text{Sm}^{3+}$  and  $\text{Dy}^{3+}$ , which exhibit multiple and crowded excitation levels, higher-level excitation induced radiationless deactivation, decreasing the probabilities and intensities of Ln/M-TNS emission. However, this behavior was not observed for Dy/Nb-TNSs. The excitation levels of  $\text{Dy}^{3+}$  (including the lowest one) are higher in energy than that of other  $\text{Ln}^{3+}$ . Therefore, the TNS-to- $\text{Dy}^{3+}$  energy transfer more hardly occurred

than other Ln/TNSs. However, Nb loading improved the TNS-to-Dy<sup>3+</sup> energy transfer, and the fluorescence intensity increased with Nb contents. Similarly, Ta loading improved the TNS-to-Dy<sup>3+</sup> energy transfer, whereas higher-levels transfer induced radiationless deactivation. Because the excitation level of Ta-TNSs was higher than those of TNSs and Nb-TNSs.

#### 4. Conclusion

The incorporation of V, Nb and Ta into TNSs affected the amount of supported lanthanides and influenced the fluorescence behavior of the resulting Ln/TNSs, with the diamond shape and water dispersibility of original TNSs remaining largely unaffected. The performed analysis showed that photodeposition involved a photo-induced redox reaction between TNSs and Ln<sub>2</sub>O<sub>3</sub>. Moreover, detailed investigation of Ln/TNS fluorescence spectra suggested that the fluorescence intensity of Ln/TNSs and Ln/M-TNSs was influenced by the overlap between the excited energy levels of TNSs and Ln<sup>3+</sup>.

#### Acknowledgement

Authors acknowledge the support of colleagues and staff of the Kawasaki Medical School. This research was supported by the Collaborative Research Project of Materials and Structures Laboratory, Tokyo Institute of Technology (26-26, 25-28) and Kawasaki Medical School Project Grants (26-B-54, 25-B-82, 25-S-5).

#### References

- [1] Tae, E. L., Lee, K. E., Jeong, J. S., and Yoon, K. B. 2008. "Synthesis of Diamond-shape Titanate Molecular Sheets with Different Sizes and Realization of Quantum Confinement Effect during Dimensionality Reduction from Two to Zero." *J. Am. Chem. Soc.* 130 (20): 6534-43.
- [2] Evans, B. L., and Young, P. A. 1967. "Exciton Spectra in Thin Crystals." In *Proceedings of the Royal Society of London A: Mathematical, Physical and Engineering Sciences* 298 (1452): 74-96. The Royal Society.
- [3] Consadori, F., and Frindt, R. F. 1970. "Crystal Size Effects on the Exciton Absorption Spectrum of WSe<sub>2</sub>." *Phys. Rev. B* 2 (12): 4893.
- [4] Dingle, R., Wiegmann, W., and Henry, C. H. 1974. "Quantum States of Confined Carriers in Very Thin Al<sub>x</sub>Ga<sub>1-x</sub>As-GaAs-Al<sub>x</sub>Ga<sub>1-x</sub>As Heterostructures." *Phys. Rev. Lett.* 33 (14): 827.
- [5] Unal, U., Matsumoto, Y., Tanaka, N., Kimura, Y., and Tamoto, N. 2003. "Electrostatic Self-assembly Deposition of Titanate(IV) Layered Oxides Intercalated with Transition Metal Complexes and Their Electrochemical Properties." *J. Phys. Chem. B* 107 (46): 12680-9.
- [6] Tsurumachi, N., Okamoto, H., Ishii, K., Kohkami, H., Nakanishi, S., Ishii, T., et al. 2012. "Formation of Aggregate in Nanohybrid Material of Dye Molecules—Titanate Nanosheets." *J. Photochem. Photobiol. A: Chemistry* 243: 1-6.
- [7] Zhang, L., Zhang, Q., and Li, J. 2007. "Layered Titanate Nanosheets Intercalated with Myoglobin for Direct Electrochemistry." *Adv. Funct. Mater.* 17 (12): 1958-65.
- [8] Zeng, Z., Yin, Z., Huang, X., Li, H., He, Q., Lu, G., et al. 2011. "Single-layer Semiconducting Nanosheets: High-yield Preparation and Device Fabrication." *Angew. Chem. Int. Edu.* 50 (47): 11093-7.
- [9] Han, X., Kuang, Q., Jin, M., Xie, Z., and Zheng, L. 2009. "Synthesis of Titania Nanosheets with a High Percentage of Exposed (001) Facets and Related Photocatalytic Properties." *J. Am. Chem. Soc.* 131 (9): 3152.
- [10] Zhang, L., Chen, D., and Jiao, X. 2006. "Monoclinic Structured BiVO<sub>4</sub> Nanosheets: Hydrothermal Preparation, Formation Mechanism, and Coloristic and Photocatalytic Properties." *J. Phys. Chem. B* 110 (6): 2668-73.
- [11] Li, H., Xie, Y., Li, K., Huang, L., Huang, S., Zhao, B., et al. 2014. "Microstructure and Wear Behavior of Graphene Nanosheets-reinforced Zirconia Coating." *Ceram. Int.* 40 (8): 12821-9.
- [12] Ohya, T., Nakayama, A., Shibata, Y., Ban, T., Ohya, Y., and Takahashi, Y. 2003. "Preparation and Characterization of Titania Thin Films from Aqueous Solutions." *J. Sol-Gel Sci. Technol.* 26 (1-3): 799-802.
- [13] Allen, M. R., Thibert, A., Sabio, E. M., Browning, N. D., Larsen, D. S., and Osteloh F. E. 2010. "Evolution of Physical and Photocatalytic Properties in the Layered Titanates A<sub>2</sub>Ti<sub>4</sub>O<sub>9</sub> (A = K, H) and in Nanosheets Derived by Chemical Exfoliation." *Chem. Mater.* 22 (3): 1220.
- [14] Yoshioka, D., Nshimura, Y., and Katsumata, K. 2017. "Synthesis and Fluorescence Properties of Lanthanide-supported Titanate Nanosheets." *J. Lumines.* 194: 316-20.
- [15] Dieke, G. H., and Crosswhite, H. M. 1963. "The Spectra of the Doubly and Triply Ionized Rare Earths." *Appl. Opt.* 2 (7): 675-86.

# The Introduction of Biofuels in Marine Sector

Theodora Tyrovol<sup>1</sup>, George Dodos<sup>1</sup>, Stamatis Kalligeros<sup>1,2</sup> and Fanourios Zannikos<sup>1</sup>

1. *Laboratory of Fuels and Lubricants, Chemical Engineering Department, National Technical University of Athens, Zografos, Athens 157 80, Greece*

2. *Hellenic Naval Academy, Piraeus, Athens 185 39, Greece*

**Abstract:** Sulphur and emissions related limits which are imposed on marine fuels drive the maritime industry to look on alternative fuels. The maximum sulphur content of the fuel has already decreased in the ECAs SO<sub>x</sub> (Sulphur Emission Control Areas) from 1.5% to 1% from 1 July, 2010, and to 0.1% from 1 January, 2015. Globally, the highest permitted sulphur content of fuel will be reduced, as from 1 January, 2020 to 0.5%. Increasing demand of low sulphur fuel is anticipated, leading to a substantial mitigation of marine fuels from residual to distillate ones. Biodiesel or else FAME (Fatty Acid Methyl Esters) and mixtures of it with conventional petroleum fuels, constitute alternative energy source for the maritime industry. The International Standard EN (European Norme) ISO (International Organization for Standardization) 8217 specifies the requirements of petroleum fuels for use in marine diesel engines. According to the previous version of EN ISO 8217:2012, distillate fuels should comply with the “de minimis level” of approximately 0.1% v/v FAME. Nevertheless, with the latest revision of EN ISO 8217 standard in 2017, the incorporation of FAME up to 7% v/v is allowed in specific marine distillate grades as DF (Distillate FAME) grades. Marine distillates can also include hydrocarbons from synthetic or renewable sources, similar to the composition of petroleum distillate fuels.

**Key words:** Alternative fuels, marine fuel, distillate fuel, ECAs (Emission Control Areas), DF (Distillate FAME) grades.

## 1. Introduction

The shipping industry is the backbone of global trade and the lifeline for island communities, transporting approximately 90% of the tonnage of all traded goods, as estimated by the International Chamber of Shipping. The energy source for the propulsion of ships has undergone significant transformations over the last 150 years, starting with sails (renewable energy) through the use of coal to HFO (Heavy Fuel Oil) and MDO (Marine Diesel Oil). The consumption of these fuels has been increasing over the years in line with the rising demand for shipping. The IMO (International Maritime Organization) estimates that between 2007 and 2012, on average, the world's marine fleet consumed between 250 and 325 million tons of fuel annually, accounting for approximately 2.8% of annual global

greenhouse gas emissions [1]. However, compared to other modes of transport, shipping produces the lowest emissions of CO<sub>2</sub> (Carbon Dioxide) per ton per kilometer travelled.

Still, emissions are expected to rise with shipping demand and they could triple by 2050 if left unregulated. On 10 October, 2008, the MEPC (Marine Environment Protection Committee) of the IMO adopted the revised MARPOL (Marine Pollution) 73/78 Annex VI on air pollution from ships. MARPOL is the International Convention for the Prevention of Pollution from Ships. The sixth Annex, which came into force on 19 May, 2005 concerns the prevention of air pollution from ships and provides the synthesis of specific emission control areas [2].

The aim of the IMO is to reduce emissions from ships by switching from heavy fuel oils to light fuel oils. The most recent regulations place restrictions on NO<sub>x</sub> (Nitrogen Oxides) and SO<sub>x</sub> (Sulphur Oxides) emissions from the seagoing ships. The MARPOL is the main international convention covering prevention

---

**Corresponding author:** Theodora Tyrovol<sup>1</sup>, chemical engineer, M.Sc., main research fields: evaluation of the lubricity of marine distillate fuels and research on alternative and renewable marine fuels.

of pollution of the marine environment from operational or accidental problems of ships. The fuel sulphur content decreases in the ECAs  $SO_x$  (Sulphur Emission Control Areas), which is the Baltic Sea, the North Sea and the English Channel, from 1.5% m/m to 1% m/m from 1 July, 2010 and 0.10% m/m from 1 January, 2015. At a global level, the highest permissible sulphur content of fuel is reduced from 1 January, 2012, from 4.5% m/m to 3.5% m/m and 0.5% m/m from 1 January, 2020.

The concentration of sulphur in marine fuel depends both on the degree of the refinement as well as on the original sulphur content of the crude oil processed by the refinery. The requirement for maximum sulphur content of 0.10% m/m in fuel oil used on board ships sailing or operating in the ECAs (Emission Control Areas) from 1 January, 2015 means in practice that it is not always effective to mix residual fuel with distillate fuel and still meet this limit in sulphur content. Recently, in an effort to combine the low sulphur content with the more preferable high viscosity of the fuel, a series of new types of fuels have been introduced which are referred to as ULSFOs (Ultra Low Sulphur Fuel Oils). However, these products are not exactly included in the relevant specifications and their availability is currently limited compared to the conventional types. Therefore, practically distillate grades as DMA (Distillate Marine grade A), DMB (Distillate Marine grade B) and DMZ (Distillate Marine grade Z) which meet the ECA sulphur requirements remain the most popular option.

## 2. Specifications of Marine Fuels

The International Standard EN (European Norme) ISO (International Organization for Standardization) 8217 sets the requirements of petroleum fuels for use in marine diesel engines and ship boilers, specifying different distillate grades (Distillate Marine or DM) and a number of residual grades (Residual Marine or RM). The previous edition of standard EN ISO

8217:2012 takes into account the main issues related to the use of low sulphur distillate fuels [3]. According to it, fuels must be deprived from biofuels except from the “de minimis” levels of FAME (Fatty Acid Methyl Esters). The “de minimis” level for distillate fuels was indicated as approximately 0.1 volume % FAME.

The demand for use of marine distillate fuels with low sulphur content has led to further research and data collection that eventually permitted the incorporation of FAME to specific grades of distillate marine fuels supplied in the marine market (DF grades). This is incorporated in the latest sixth edition of ISO 8217:2017 which was put into force earlier this year [4]. Eventually, new types of 0.1% S (Sulphur) fuels are entering the market in response to the 0.1% S ECAs  $SO_x$  limit [4]. The sixth edition on the EN ISO 8217 standard includes additional requirements for distillate fuels to protect against cold operability issues as well. Hence, it offers improved quality control and better protection against operational issues while the introduction of DF grades improves fuel oil availability in specific ports.

FAME has previously been regarded as a contaminant in all marine fuels, but the new grades allow bio-fuel blends containing up to 7% v/v FAME. Marine distillates can also include hydrocarbons from synthetic or renewable sources, similar to the composition of petroleum distillate fuels.

## 3. Alternative Fuels in Marine Industry

The incorporation of biofuels in the marine distillate fuels is still one of the major options for the transition to a smarter and greener transport system with low carbon footprint. Biofuels have already entered the market, driven amongst other by their potential to improve energy security and to contribute to climate change mitigation.

Biofuels are one of the few technologies currently available that have the potential to substitute oil and

provide benefits to the transportation system. Biofuels on their own cannot deliver a sustainable transport system and must be developed as part of an integrated package of measures, which promotes other low carbon options and efficiency, as well as moderating the demand and need for transport [5].

Biofuels are usually categorized as first, second and third generation, based on the technology and/or the raw materials that are utilized for their production. In first generation biofuels, the carbon source comes from sugar, lipid or starch which is directly extracted from a plant. In this category, the following are included: biodiesel, vegetable fats, biogas, bio-alcohols and synthetic gas. First generation biofuels can offer substantial CO<sub>2</sub> benefits and can help to improve domestic energy security. The production of 1st generation biofuels is commercial today, with almost 50 billion liters produced annually. Nevertheless, 1st generation biofuels seem to create great concerns about the environmental impacts and carbon balances—reasons that set remarkable limits in their production. The main disadvantage of first generation biofuels is the food-versus-fuel debate and one of the major reasons for rising food prices is due to the increase in the production of these fuels. Additionally, biodiesel is proven to be a non-cost-efficient emission abatement technology [6].

Second-generation biofuels can be broadly grouped into those produced either biochemically or thermochemically, either route using non-food crops, especially from lignocellulosic feedstocks sourced from crop, forest, or wood process residues, or purpose-grown perennial grasses or trees. Such crops are likely to be more productive than most crops used for 1st generation, in terms of the energy content of the biofuel produced annually per hectare (GJ/ha/yr) [7]. In the second-generation biofuels, the following are included: methyl esters derived from used cooking oils, bio-oil, butanol, mixed alcohols, lignocellulosic alcohol and HVOs (Hydrogenated Vegetable Oils). It is anticipated that 2nd generation biofuels could

significantly reduce CO<sub>2</sub> emissions. Moreover, they do not compete with food crops and some types of them can offer better engine performance [8].

Third-generation biofuels are based on improvements in the production of biomass. This technology takes advantage of specially engineered energy crops such as algae as its energy source. The algae are cultured to act as a low-cost, high-energy and entirely renewable feedstock. Algae can be grown using land and water unsuitable for food production, therefore, reducing the strain on already depleted water sources.

Liquid biofuels that are under consideration generally in the marine section and specifically in this work are biodiesel—FAME, HDRD (Hydrogenation Derived Renewable Diesel) or HVO and synthetic diesel BTL (Biomass to Liquid). Both HVO and BTL are high quality synthetic renewable diesel fuels.

### 3.1 Biodiesel or FAME

Biodiesel, which is defined as the monoalkyl esters, mainly methyl esters (FAME), of long-chain fatty acids derived from renewable biological sources, such as vegetable oils or animal fats or waste cooking oils by transesterification, is considered as a possible substitute or extender of conventional diesel fuel. Biodiesel should comply with the requirements set by EN ISO 14214 which is a standard developed only for FAME.

Due to its polar nature, biodiesel is considered to be a lubricity improver and increases the lubricating efficiency of low sulfur marine fuels. Therefore, it reduces the wear of the components of the fuel delivery systems. On the other hand, it can degrade over time forming contaminants in the form of peroxides, acids and other insoluble particles. Biodiesel, especially in higher concentrations, can dissolve certain nonmetallic materials such as seals, rubber hoses and gaskets. It can also interact with certain metallic materials, such as copper and brass.

For an existing ship, the fuel system and engines may have to be modified by changing out susceptible parts with biodiesel—compatible components for safe operation.

### 3.2 Synthetic Biofuels

Synthetic biofuels are defined as fuels that are synthesized predominantly from synthesis gas produced by cleaned and modified gas from thermal gasification (such as partial oxidation) of biomass. Synthetic fuels have several advantages because they can be used without modification in the existing engines and fuel supply. In addition, synthetic biofuels are considered cleaner than traditional fuels due to the removal of all contaminants so to avoid poisoning the catalysts used in the processing [9].

There are several thermal and chemical processes that can be used to produce synthetic hydrocarbons. The main routes are:

Thermal gasification to syngas (a mixture of hydrogen and carbon monoxide) followed by upgrading by FT (Fischer-Tropsch) synthesis;

Thermal gasification followed by methanol synthesis upgrading with MTG (Methanol to Gasoline) or MOGD (Methanol to Olefins, Gasoline and Diesel) processes;

Fast pyrolysis for gasification and subsequent upgrading of the syngas;

Fast pyrolysis followed by upgrading by hydro-processing or zeolites;

Hydro-processing which uses hydrogen to remove oxygen and other contaminants such as sulphur and nitrogen from vegetable oil.

#### 3.2.1 HVO

Hydrotreating of vegetable oils is a modern way to produce high-quality biobased diesel fuels without compromising fuel logistics, engines, exhaust aftertreatment devices or exhaust emissions.

Hydrotreating of vegetable oils as well as suitable waste and residue fat fractions to produce HVO is a quite new but already mature commercial scale

manufacturing process. In this process, hydrogen is used to remove oxygen from the triglyceride vegetable oil molecules and split the triglyceride into three separate chains, creating hydrocarbons which are similar to petroleum diesel fuel components. This allows blending in any desired ratio without any concerns regarding the fuel properties.

Figures published by the “RED” (Renewable Energy Directive) 2009/28/EC show that life cycle greenhouse gas emissions of HVO are slightly lower than those of FAME if both are made from the same feedstock [10].

Chemical HVOs are mixtures of paraffinic hydrocarbons and are free of sulphur and aromatics with considerably high cetane number and good oxidation stability [11]. It has the highest heating value of the existing biofuels and low tendency to form deposits in the fuel injection system. In those cases, an isomerization stage is included. HVO has no cold operability issues with severe winter grades.

On the other hand, compared to FAME, there are few companies that have invested to produce hydrogenation derived renewable diesel, and eventually, its current availability is still low. HVO as well as BTL should meet the specifications contained in EN 15940 for paraffinic diesel fuels.

#### 3.2.2 BTL

BTL is a process that transforms biomass to a usable form of biofuel. The production process is based on FT synthesis for converting lignocellulosic biomass into synthetic liquid hydrocarbons.

A great advantage of BTL is the fact that when burned, it does not produce non-renewable carbon dioxide. Therefore, BTL is carbon dioxide neutral and has no impact on the enhanced greenhouse effect. BTL can be blended with marine distillate fuel, according to EN ISO 8217-2017, but there is more experimental research to be done concerning the optimum ratio of biofuel and marine distillate fuel that will be aligned with the requirements of EN ISO 8217.

#### 4. The Use of FAME, HVO and BTL in Marine Distillates

The percent of ester-type biodiesel fuel (e.g. FAME derived from used cooking oil) that can be added to a marine distillate fuel is up to 7% v/v. Neat biodiesel contains almost no sulphur, so SO<sub>x</sub> exhaust emissions are practically zero. Biodiesel blended with marine distillate fuel at a predetermined percentage (up to 7% v/v) leads to remarkable improvement of the conventional marine fuels' lubricity. The increasing addition of biodiesel in marine distillate fuel brings significant improvement in the cetane index of the resulting blends and in their ignition point. With the percentage increase of biodiesel mixed with the conventional marine fuel, the sulphur content of the mixture is considerably reduced. The cold flow properties of the blends (cloud point, pour point and CFPP (Cold Filter Plugging Point)) are slightly comprised by the addition of increasingly quantity of biodiesel, since a slight increase in these properties is observed [12].

The great concern with biodiesel lies among the variant quality of the biofuel, the impact of the fuel system components, the possible loss of the engine manufacturer's warranties, the unfavorable hygroscopic properties, the impact on the cold flow parameters and the limited long-term storage stability [13].

By blending 10% of HVO into marine distillate fuel, quality is not compromised while it reduces exhaust emissions and enhances engine operation. In fact, the fuel blends are proven to be of premium grade since their cetane number is increased and the aromatic content is decreased, resulting in reduced exhaust emissions and satisfactory cold-start performance. HVO fuel also contains almost no sulphur, so the SO<sub>x</sub> exhaust emissions are practically zero. When blended with marine distillate fuel in increasing proportions, it lowers the sulphur content of the mixtures. HVO fuel meets the diesel fuel specification and is as safe as the diesel fuel. The cold flow properties in the case of

mixtures of marine distillate fuel with HVO are remarkably improved since by gradually mixing marine distillate fuel with hydrogenated vegetable oil, the resulting mixtures exhibit better cold properties and they can be used in more severe conditions.

The lubricity of neat HVO corresponds to that of sulphur-free fossil diesel and GTL (Gas to Liquid) diesel fuels. Without any lubricity additives, the HVO does not meet the HFRR (High Frequency Reciprocating Ring)-ISO 8217 requirement of < 520 µm for protecting fuel injection equipment against wear. So, when blended with marine distillate fuels, it cannot enhance the lubricity of the resulting mixtures. As it is already mentioned, FAME addition is proven to amend lubricity properties in ultra-low sulphur marine distillate fuels. This trade-off in marine distillate's properties for blends with FAME and renewable diesel is indicative that both fuels could be used simultaneously and complement each other in marine diesel fuel blends.

Both HVO and BTL are paraffinic diesel fuels with several fuel advantages over transesterified lipids. HVO and BTL have higher cetane number, implying easier ignition and more efficient combustion, better storage stability, better cold properties and less tailpipe NO<sub>x</sub> emissions. They also have higher renewability fraction of the fuel (97%-98% and renewable mass inputs versus 90% renewable mass inputs of transesterified lipids). In case HVO is produced from waste feedstock with low upstream impacts, the high conversion efficiency of the HVO production process will make HVO the preferred fuel to BTL from any woody feedstock, even woody waste.

#### 5. Conclusion

Strict regulations on emissions and reports on harmful effects associated with the use of traditional marine fuels are driving the marine industry to adopt alternative fuels. Many ship operators, with present-day propulsion plants and marine fuels, cannot

meet the new regulations without installing expensive exhaust after treatment equipment or switching to low-sulfur diesel, ultra-low-sulfur residual or alternative fuels. All of them contain properties that reduce engine emissions below mandated limits but impact bottom-line profits.

Thus, the search for alternative fuels which will satisfy fully or partially the new emission regulations and sulfur limits without compromising the economy, has been brought to limelight worldwide.

The shipping industry is starting to understand the potential of truly sustainable biofuels as an emerging solution. Driven by both regulatory and market factors, biofuels could make up 5-10% of the total global marine fuel mix by 2030. For the market to properly embrace marine biofuels as a viable long-term solution, they must be comparable and compatible with current shipping fuels. They must also be truly sustainable, adhering to principles concerning all aspects of the biofuel chain, including the environmental, social, legal, local and global effects of biofuel extraction, production and delivery.

The commercial marine use of biodiesel involves compression ignition engines, boilers and gas turbines. Biofuels are sulphur-free; thus, their uses can reduce the SO<sub>x</sub> problem from shipping. The emissions of particulate matter will be also significantly reduced resulting in a reduced health risk and finally only renewable CO<sub>2</sub> will be emitted during combustion.

The increased awareness of human induced environmental crisis has created an interest in using cleaner renewable energy instead of fossil fuels. Marine transport is one of the sectors with the fewest available alternatives to fossil fuels [14]. On a technical level, the introduction of alternative fuels is accompanied by additional complexity, in the areas of fuel supply infrastructure, rules for safe use of fuels on board and operation of new systems. Over the last years, barriers for biofuels deployment have moved from the biofuels technology to policy and financing. Commercialization depends on political leadership

and adequate policies. It is recognized that innovative energy technologies are not yet cost-competitive against conventional biofuels and fossil fuels, which they aim to displace.

## References

- [1] Acciaro, M., Hoffman, P. N., and Eide, M. S. 2013. "The Energy Efficiency Gap in Maritime Transport." *Journal of Shipping and Ocean Engineering* 3 (1-2): 1.
- [2] TOCPRO. 2015. *MARPOL 73/78 Practical Guide 2015, International Convention for the Prevention of Pollution from Ships*. Accessed January 4, 2016. <https://maddenmaritime.files.wordpress.com/2015/08/marpol-practical-guide.pdf>.
- [3] Technical Committee ISO/TC 28/SC 4, International Organization for Standardization. 2012. *International Standard ISO/FDIS 8217:2012: Petroleum Products—Fuels (Class F)—Specifications of Marine Fuels* (5th Edition). ISO, 1-36.
- [4] Technical Committee ISO/TC 28/SC 4, International Organization for Standardization. 2017. *International Standard ISO/FDIS 8217:2017: Petroleum Products—Fuels (Class F)—Specifications of Marine Fuels* (6th Edition). ISO, 1-23.
- [5] McGill, R., Remley, W., and Winther, K. 2013. "Alternative Fuels for Marine Applications." *A Report from the IEA Advanced Motor Fuels Implementing Agreement*: 54.
- [6] Mofor, L., Nuttall, P., and Newell, A. 2015. "Renewable Energy Options for Shipping, Technology Brief." *IRENA (International Renewable Energy Agency), Bonn*.
- [7] Eisentraut, A. 2010. *Sustainable Production of Second-Generation Biofuels, Potential and Perspectives in Major Economies and Developing Countries: Information Paper*. OECD/ IEA (International Energy Agency).
- [8] Sims, R., Taylor, M., Saddler, J., and Mabee, W. 2008. "From 1st to 2nd Generation Biofuel Technologies: An Overview of Current Industry and RD & D Activities." *International Energy Agency*: 16-20.
- [9] Bruining, E., Elens, R., Roos, E., Slingerland, J., and Torre, C. V. 2015. "Synthetic Fuels for Global Shipping." *Rotterdam Mainport University*, 1-36.
- [10] European Union. 2009. "Directive 2009/28/EC of the European Parliament and of the Council of 23 April 2009 on the Promotion of the Use of Energy from Renewable Sources and Amending and Subsequently Repealing Directives 2001/77/EC and 2003/30/EC." *Official Journal of the European Union* 5.
- [11] Engman, A., Hartikka, T., Honkanen, M., Kiiski, U., Kuronen, M., Lehto, K., et al. 2016. "Neste Renewable

- Diesel Handbook.” Neste Corporation.
- [12] Tyrovola, T., Dodos, G., and Zannikos, F. 2017. “The Effect of FAME and HVO on Oxidation Stability, Cold Properties and Lubricity of Marine Distillate Fuels.” 11th International Colloquium Fuels, TAE (Technische Akademie Esslingen).
- [13] Florentinus, A., Hamelinck, C., van den Bos, A., Winkel, R., and Cuijpers, M. 2012. “Potential of Biofuels for Shipping.” *ECOFYS, Netherlands BV, Utrecht*.
- [14] Rahman, A., and Mashud, K. 2015. “Overview of Alternative Fuels and Their Drivers to Reduce Emissions in the Shipping Industry.” In *International Conference on Mechanical and Industrial Engineering (ICMAIE’ 2015)*, Kuala Lumpur.

# Economic Analysis of the Internalization the Externalities in Environmental Goods

Odysseas Kopsidas and Andreas Hadjixenofontos

*Department of Economics and Business, School of Economics and Business, Neapolis University Paphos, Paphos 8042, Cyprus*

**Abstract:** The environment is characterized as a public good. Public goods are goods that provide benefits for society as a whole or part of it, usually regardless of whether the individual people are willing to pay to have these benefits. This proposed project is not viable in profitable terms to private enterprise, so it applied a modified version of the CVM (Contingent Valuation Method) to realize this project. The purpose of the paper is to present a modified model of an internalizing external costs caused by the operation of a manufacturing unit in conjunction with the new reality created. Using the CBA (Cost-Benefit Analysis), all critical parameters problem attributed to a single base assessment, which facilitates decision making process. The basis of evaluation is to compare benefits and costs. It is used the CVM in case study and the results show that there is less sensitivity for restoration of the cultural heritage monuments in comparison with the sensitivity for restoration of the natural and urban environment in general.

**Key words:** Experimental economics, WTP (Willingness To Participate), information, questionnaire.

## 1. Introduction

The purpose of this work is to present a modified model of internalization the external costs caused by the operation of a manufacturing unit in conjunction with the new reality created. The environment is characterized as a public good. Public goods are goods that provide benefits for society as a whole or part of it, usually regardless of whether the individual people are willing to pay to have these benefits. All entities, whether individuals or businesses or public agencies, have some financial resources with which they seek to achieve specific objectives (e.g. profit maximization) [1, 2]. To achieve a specific objective, usually there are many alternatives and possibilities. To be effective, i.e. to utilize the existing resources in the best manner possible, should be selected that the solution maximizes the desired outcome or minimizes the required sacrifices [3].

The procedure for the selection process is called optimization or maximization. In the business world, almost all the decisions may be considered as

optimization problems. The optimization can be applied to maximize the profit and minimize the cost of production [4].

## 2. The Problem Formulation

The optimization without constraints means that a business seeks to maximize the benefits or minimize costs without putting constraints on resources that will be used. The optimization effort can be not only one but several things simultaneously, so the problem becomes more complicated. There is a problem with optimization constraints when seeking to maximize utility or minimize the cost of an activity with the restriction that is certain pore size to be placed. The individual seeks to maximize his own benefit, cares only for his private benefits and costs and is utterly indifferent to the consequences of acts of other members of society. The relationship between risk and expected return is the key to whether or not to an investment [5].

Often, projects or activities have external effects, which involve social costs or benefits, in addition to the private external influences, because they are internalized in market prices and create tension

---

**Corresponding author:** Odysseas Kopsidas, Ph.D., main research field: environmental economics.

between market prices and social benefits or costs. The economic analysis or CBA (Cost-Benefit Analysis) identifies and quantifies the benefits and costs of an activity or policy, and considers whether it is appropriate and beneficial implementation of the whole economy and society.

To properly place a CBA should make all sizes reflect the image of society. The various inputs and outputs that occur on a project from markets can function effectively or not. When markets function efficiently, the use of the purchase price is good approximation of the social cost. When you come from markets which are not operated effectively, the price does not reflect the true social costs on them [6].

### 3. Methodology

Using the CBA, all critical parameters problem attributed to a single base assessment, which facilitates decision making process. The basis of evaluation is to compare benefits and costs. If the benefits are larger, then the project (or activity) is socially desirable. "Weak" Treaty Pareto is that a project or a policy measure is socially acceptable when improving the welfare of every member of society. "Strong" condition Pareto is that a project or a policy measure is socially acceptable when ensure improved welfare even one person without reducing the welfare of another. The Pareto principle is based on individual conception of welfare, whereby the people regarded as the best exponents of their own prosperity through their options. It has limited use, since there is almost no action to improve [7, 8].

The search for suitable instruments or for the best possible combination of the use of command and control and of economic instruments nowadays constitutes one of the most complex points of discussion on environmental economics. The environmental reassessment of economic procedures and the change in production and consumption of non-conservation friendly models, which constitute the fixed position of the EU (European Union) and the

OECD (Organisation for Economic Co-operation and Development), could be achieved by using suitable economic instruments. Authors are focalising the present study on environmental taxes, the most well-known and widespread category of economic instruments, by studying the advantages and disadvantages of their enforcement. Next, authors will present the experience at an international level, focusing on their use as well as the consequences on international competitiveness.

According to the first theorem of economic prosperity, under certain conditions, a competitive economy guarantees a Pareto-optimal economic outcome. In other words, a competitive market leads to allocations of resources to the property that any position cannot improve or worsen the position of another. This allocation is done automatically through the price mechanism, e.g. where there is a demand, the price goes up and when there is a bid price, it falls. The adjustment of prices solves the problem of distribution of goods. The second fundamental theorem states that through the competition of firms that have objective, the maximization of profits and consumers who view they maximize the benefits can be excellent distribution of resources regardless of the initial distribution. Therefore, it is necessary to have a central designer to decide who gets what in the economy. In fact, the free market can lead to great disparities that can be removed by state intervention (e.g. taxation).

### 4. Problem Solution

The externalities or the external economies occur when a person acts or a business affects other people or companies when a company imposes a cost on others but does not compensate, or end, or when a company brings benefits in other businesses but does not receive remuneration for providing this benefit. It is distinguished two types of externalities, public e.g. air pollution, the water that affects the welfare of many people and private e.g. a person casts trash in

the yard of neighbour (This movement affects the welfare of the neighbour and any other). The cases where the activity of an individual or business imposes costs on others refer to as negative externalities or external costs. When positive externality is induced in the production of a commodity, the social costs production is less than the private cost. The optimal quantity of good 'Q' optimum is greater than the equilibrium quantity 'Q' market. Notice that in both cases, it is used for either external charges, or external economies; the price mechanism does not give enough information to the recipient of decisions. In one case, the values do not represent the actual cost and the other does not represent a real benefit. It is said market failure. According to Classic Economic Theory, taxation is an effective tool for addressing the external charge. Unlike the modern economics is as a way of supporting externalities awarding property rights over natural resources. It is argued that if the contaminant obtains a right of victims of pollution, then pollution will pay the first to stop or reduce the polluting activity. Unlike the pollutants to be able to benefit from the natural resource should compensate the victims, which have acquired the right to operate.

When there is a clearly defined system of property rights, the market mechanism will lead to an efficient allocation of resources. In environmental policy, the polluter (whether company or individual, or the State) pays applicable in several countries in the world. This is automatically an incentive to reduce pollution at least at the level where the marginal cost of reducing pollution equals the marginal cost of damage causing this pollution. Also, many countries apply the system of subsidies for the pollution control. This suggests that property rights are particularly important in the formation of environmental policy.

Economic theory emphasizes the importance of ownership of natural resources and negotiations between those resources which pollute and those who suffer from pollution. In particular, the passage of

regulatory approach to environmental protection, which was based mainly on the use tools of direct intervention on the strategic and integrated approach, requires an overall strategy for sustainable development.

Environmental redefinition of economic processes and changing unsustainable patterns of production and consumption cannot be achieved with tools to intervene directly, but rather the use of economic tools. The same should be accepted and to solve the environmental problems of the second generation, such as climate change, biodiversity loss and soil erosion, as taking effective measures in this direction requires the use of other tools except those of direct intervention. The key feature of economic instruments is that the type of conduct which guides the operators of production processes associated with a particular economic advantage. The logic function consists in particular to internalize partially or completely, of externalities i.e. the impact on the environment, which is secondary effect of production processes and consumption and which is not calculated as a cost to those who cause it. This is also an established position in economic theory. It should also be noted that all financial instruments do not show the same degree of compatibility with the market mechanisms.

These tools provide economic incentives for environmental change behaviour either through direct changes in the levels of prices and costs through fees products, duties on carbon or on raw materials, or through indirect changes in prices or the costs through financial and fiscal instruments such as direct subsidies, loans or ending through creating new markets for environmental goods, such as tradable licenses, etc.. The production and consumption of goods and services have created adverse impacts on the environment. Starting thus with the principle "I live, so be foul" and realizing that one cannot speak for the elimination of pollution, the problem lies in "how much pollution". In other words, what will be the "optimum" level of environmental pollution or

environmental protection from pollution, based on various economic, technological, social, psychological and other parameters that apply to a society in a given period?

The environmental degradation may be defined in economic terms, as external costs. The internalization of these costs occurs when polluters pay a tax or a fee. A tax or fee is defined as the payment for each unit of pollution deposited degradation. The main economic reason for using taxes in environmental policy is the integration of the costs of pollution and any other use of the environment on commodity prices and services produced by economic activities. Such costs are called 'externalities', because they are side effects of economic activity and not part of the prices paid by producers or consumers who are directly involved. The calculation of the economic value of externalities is not easy. For example, recent calculations show that the external environmental costs of road transport, such as increased costs resulting from air pollution, climate and disturbance from noise are quite large and growing.

These 40 externalities cost the EU an average of about 5.5% of GDP (Gross National Product). If you include the costs associated with accidents, costs are as high as 7.8% of GDP. An environmental tax tries to incorporate these external costs on prices ('internalising externalities') so that both social and private costs come closer. The better prices allow the markets to work more efficiently, leading to a reallocation of resources under 'fair and efficient' prices through the redistribution of costs. Environmental taxes also help in implementing the principle 'the polluter pays', after facing those who cause pollution to the full costs of polluting their activity. In practice, there is little or no agreed data on the economic costs of externalities or their distribution and therefore, the people making policies determine the price environmental taxes on those levels that they believe will achieve their goals of their policy.

The impact of environmental taxes on

competitiveness is an issue which is constantly on the agenda of discussions. The potential adverse effects on international competitiveness concern to designers of environmental policy when considering their application in energy and other products related to environmental problems. Some factors affecting the efficiency of environmental policy and effects on international trade are the size of its economy and its influence on pricing internationally.

The solution of environmental problems was used in system direct control (strategy command and control). The inability of the system for control and imposition of rules by the State in conjunction with the economic inefficiency characterizing the system cost of pollution control, led to the shift environmental policy, adopting economic tools to solve them. According to experience so far, financial tools can act as flexible, efficient and effective mechanisms under certain circumstances to achieve environmental objectives.

## 5. Case Study

The size of the external economy is estimated approximately by the method of the CVM (Contingent Valuation Method). The CVM is a survey-based technique, frequently used in experimental economics, especially useful for the valuation of non-market resources/goods/services and cultural heritage objects (of aesthetic, historic, scientific or social value), such as conservation of monumental remains and preservation of the physical and anthropogenic environment. The basic dependent variables used in CVM are (i) WTP (Willingness To Pay), which is the maximum monetary amount that an individual would pay to obtain/preserve a good; and (ii) WTA (Willingness To Accept) compensation, which is the minimum monetary amount required to relinquish the good. Therefore, WTP provides a purchase price, relevant for valuing the proposed gain of the good while WTA provides a selling price, relevant for valuing the proposed loss of the good. According to

classic economic theory, a significant difference between WTP and WTA should not occur, on condition that there is (i) no transaction cost; (ii) perfect information about goods/services and corresponding prices; (iii) no income effect; (iv) a market that engenders truthful revelation of preferences. Although these conditions were generally met in several economic experiments that used inexpensive market goods with readily available substitutes, the ratios WTA/WTP obtained were significantly greater than unity. This result was attributed to the fact that participants in these experiments lacked market experience.

In case that the CVM is applied for monumental remains, certain specific problems arise, because (i) the 'good' under examination has a subjective value, dependent on the cultural level of each reviewee; (ii) the intangibles associated with this 'good' are related to the present political behavior of each individual as regards his/her attitude to the local authorities or the central government; (iii) as a result, the answers may be biased, a matter that becomes evident only after final statistical processing, thus calling for supplementary information, possibly by means of an additional post-questionnaire; and (iv) the adopted/developed (for elicitation of people's WTP) technique itself should be revised (possibly by means of a meta-questionnaire) by the same group of experts who processed the answers in order to improve the questionnaire and store it into a dedicated KB (Knowledge Base) for future usage, since each monument is unique and the results coming from examining quasi-similar cases are of limited value.

## 6. Results

The sample N-valid is 100 responses regarding the WTP and N-missing is null. The descriptive statistics provide helpful information on the percent frequency of the WTP-value: 36% of the sample suggested WTP = 0 €, 16% agreed with WTP = 1-10 €, 10% accepted WTP = 11-50 €, 20% mentioned WTP = 51-100 €,

while 18% was willing to pay > 100 €.

One of the principle descriptors investigated in the main study concerns  $X_5$ , i.e., the preference of the interviewees about the options (i) leave the situation as it is; (ii) perform only the necessary remediation; or (iii) proceed with radical restoration. Option (i) has been selected only by 12.5% of those that stated WTP = 1-10 €, which gives a 2% of the total sample. Option (ii) is agreed by 51% of the total sample, i.e., 61.1% of those with WTP = 0, 37.5% of those with WTP = 1-10, 40% of those with WTP = 11-50, 70% of those with WTP = 51-100 and 27.8% of those with WTP > 100. Option (iii) has been proposed by 47% of the interviewees, i.e., 38.9% of those with WTP = 0, 50% of those with WTP = 1-10, 60% of those with WTP = 11-50, 30% of those with WTP = 51-100 and 72.2% of those with WTP > 100.

It is worthwhile noting the relation between WTP and preference on restoration options. The interviewees that are willing to pay significant amounts tend to prefer a mild intervention, while those that agree with minimal to null amounts demand radical intervention. The latter group also considers any contribution of theirs to restoration as unfair judging that this expenditure should be covered exclusively by the State. From a socio-psychological point of view, this attitude may reflect extreme personalities with a tendency to holistic and pure solution (i.e., no mixed strategy involving people and the State is acceptable by interviewees who considered themselves as having no further obligations after regular tax-paying); as a result, they think that the State is exclusively responsible to resolve the situation.

In the case of restoration of the natural environment at three lakes in northern Greece, the WTP method is used to compute approximate external economies. The preservation/restoration of natural environment is frequently entailing excessive cost (paid by people through taxation), while it is a source of additional income for both, the State and the people, due to tourism. Since the evaluation of this good cannot be in

market terms, it is applied here in a modified version of the CVM, which is used in experimental economics in order to investigate the significance that people put on this good and how much they might be willing to pay for supporting activities concerning the preservation/restoration of Lake Kastoria. The WTP depends on (i) external diseconomies; (ii) the expectations for property values' rise as a result of the restoration; (iii) the proximity of interviewees' residence to the lake; (iv) the opinion of the interviewees; and (v) the time and money the interviewees spent for visiting the lake.

The survey sample consisted of 51.25% women and 48.56% men, the majority between 26 and 35 years old, since young people were more willing to participate in the survey; 27.5% of the respondents hold a university degree, whereas 37.50% had high school education. The majority of the interviewees belonged to the intermediate income class and enjoyed full-time employment. About 50% of the respondents live or work in close proximity of the lake; however, average WTP does not differ significantly with proximity or distance. Given that extensive media coverage during the recent years, most people were well aware about the problems of the lake. When respondents were asked to assign a level of importance to the protection of the lake on a 3-point scale (very, enough and slightly), 93.75% placed it at the highest scale, 11.25% at the medium scale and only 5% at the lowest.

The survey examined, among other factors, the attitude of citizens towards the general environmental problems of the area and the benefits that would derive from restoring the lake's ecosystem. The majority of the interviewees allocate the responsibility of environmental degradation to the failure or limited capacity of the State and local authorities, whereas they support all of the restoration activities proposed, with 69.03% giving high priority to biological agriculture for decreasing the input of chemical contaminants.

Economic valuation is a two-part process in which the first part (demonstration) displays and measures the economic value of environmental assets, while the second part (appropriation) finds ways to capture the value. The present survey has managed to demonstrate the economic value of preserving Lake Kastoria; the appropriation of this value requires policies, rules and regulations on the part of concerned agencies and institutions.

The WTP, a so-called 'restoration fee', which is actually a 'user's fee', indicates the possibility of fund raising from the community, especially when lake restoration is linked to tourist economy. On the other hand, non-use values for the lake, which this study shows to be substantial, can be captured through appropriate policy instruments. Designing appropriate policy instruments is one big task in itself and there are possible options to be considered like voluntary contribution or council taxation. Since education is a determinant that increases WTP in the medium/long-run, future surveys should target schools, colleges, and universities in the area, so as to increase potential 'capturable' non-use values and acquire relevant information useful for sensitizing young people.

In conclusion, in this analysis, it is demonstrated that social science research can provide useful information for complex environmental policy problems such as the restoration of a lake system. Policy analysis for such cases is especially difficult because these systems provide multiple, interdependent services that vary by type of lake, location, ecohydrological management and other factors. The work presented herein has been proven a useful comprehensive tool for determining the realistic cognitive burden for stakeholders and third parties.

In the case of restoration of the natural environment in industrial areas on the outskirts of Athens, the method is used to calculate WTP external economies as well. So during the last three decades, there has been growing interest in developing methods for assessing the preferences (of experts, stake holders,

community/organization members and independent individuals) for environmental quality.

This framework described above has been implemented in three cases at sites close to Athens (Lat. 37°58'42.22" N, Long. 23°43'01.12" E), referring to (i) the towns/ports Agioi Theodoroi (50.94 km south of Athens, Lat. 37°55'44.55" N, Long. 23°08'25.96" E) and Khalkis (54.87 km north of Athens, Lat. 38°27'47.06" N, Long. 23°35'29.78" E), where the source of pollution is an oil refinery and a cement production unit, respectively; and (ii) the small industrial city/port (actually a suburb 18.04 km to the south of Athens) of Eleusina (Lat. 38°0.2'36.09" N, Long. 23°32'31.63" E), where there are several sources of pollution.

In the town of Agioi Theodoroi, a quarter of the interviewees behave in an absolutely passive mode, while the rest exhibit a consistent attitude willing to pay or accept a rather small amount of money; nevertheless, 35% of them are in favor of relocation, possibly because they have interests with real estate or business associated with tourism. In the town of Khalkis, although 37% of the interviewees are not willing to pay, the corresponding percentage for WTA is negligible while the rest WTA-percentages are considerably high and in good agreement with the results for WTR (Willingness To Relocate).

In the small city of Eleusina, the absolutely passive percentage is quite high for both, WTP and WTA (46% and 67%, respectively), but 47% of the interviewees are in favor of relocation; this can be attributed to the high price of land in this suburb of Athens; the interviewees think they can take advantage from changing the use of land from industrial to urban, while they believe that the industrial units, where most of the inhabitants work, will relocate to a nearby place, quite accessible without entailing excessive transportation cost.

## 7. Discussion and Concluding Remarks

In this paper, it is considered that the natural

environment as a public good and environmental pollution as an external economy fails the price mechanism to internalize. In all three cases, the approach of foreign trade was with the CVM and calculated the external costs generated by the degradation of the environment from the responses of respondents in monetary units. Respondents answered without knowing it was the environment to its original condition and did not expect it to return to its original form. In the case of archaeological monuments, residents have built their buildings. In case of lakes, respondents have developed an urban way of life around the lakes. In the case of industrial units, residents have supported throughout the local economy on them. The initial state of the environment is unknown and undefined. Human works and buildings create new values in the region and therefore, the external costs can be measured only with the expected quality of the environment and this is not lost. Allowances, taxation and value of land use are calculated solely on the expected image of the landscape.

Therefore, the Pareto optimal socioeconomic lines status is defined according to the new form of environment created after the regeneration of areas and not according to the initial state of the environment. In any case, the society wants to reach the minimum point of the charge received from the pollution and what can be achieved by the 'invisible hand', but the regulation and government intervention. History has shown that the charge received by the society, because of pollution varies with the socioeconomic status of citizens. The more low-income residents are, more elastic the loss of the natural environment is.

## References

- [1] Bedate, A., Herrero, L. C., and Sanz, J. A. 2004. "Economic Valuation of the Cultural Heritage: Application to Four Case Studies in Spain." *Journal of Cultural Heritage* 5 (1): 101-11.
- [2] Hanemann, W. M. 1991. "Willingness to Pay and Willingness to Accept: How Much Can They Differ?"

- The American Economic Review* 81 (3): 635-47.
- [3] Bateman, I., Munro, A., Rhodes, B., Starmer, C., and Sugden, R. 1997. "A Test of the Theory of Reference-dependent Preferences." *The Quarterly Journal of Economics* 112 (2): 479-505.
- [4] Horowitz, J. K., and McConnell, K. E. 2003. "Willingness to Accept, Willingness to Pay and the Income Effect." *Journal of Economic Behavior and Organization* 51 (4): 537-45.
- [5] Brown, T. C. 2005. "Loss Aversion without the Endowment Effect, and Other Explanations for the WTA-WTP Disparity." *J. Econ. Behav. Org.* 57 (3): 367-79.
- [6] Liao, T. F. 1994. *Interpreting Probability Models: Logit, Probit, and Other Generalized Linear Models*. LA: Sage Publications Inc..
- [7] Menard, S. 2001. *Applied Logistic Regression Analysis* (2nd ed.). LA: Sage Publications Inc..
- [8] Kopsidas, O., and Batzias, F. 2011. "Improvement of Urban Environment and Preservation of Cultural Heritage through Experimental Economics by a Modified Contingent Valuation Method (CVM)." *Recent Researches in Energy, Environment, Devices, Systems, Communications and Computers*: 157-62.

# Call for Papers

Dear author,

This is *Journal of Environmental Science and Engineering* A (ISSN 2162-5298) and *Journal of Environmental Science and Engineering* B (ISSN 2162-5263) (Earlier title: Journal of Environmental Science and Engineering, ISSN 1934-8932), a professional journal published across the United States by David Publishing Company, New York, NY 10034, USA.

*Journal of Environmental Science and Engineering* A (ISSN 2162-5298) and *Journal of Environmental Science and Engineering* B (ISSN 2162-5263) (Earlier title: Journal of Environmental Science and Engineering, ISSN 1934-8932) is collected and indexed by the Library of US Congress, on whose official website (<http://catalog.loc.gov>) an on-line inquiry can be triggered with its publication number ISSN 2162-5298 and ISSN 2162-5263 as key words in “Basic Search” column. In addition, these journals are also retrieved by some renowned databases:

- Google Scholar
- Chinese Database of CEPS, Airiti Inc. & OCLC
- Chinese Scientific Journals Database, VIP Corporation, Chongqing, P.R. China
- CSA Technology Research Database
- Ulrich’s Periodicals Directory
- Summon Serials Solutions
- CAS (Chemical Abstracts Service)
- CiteFactor (USA)
- Proquest

David Publishing strives hard to provide the best platform for researchers and scholars worldwide to exchange their latest findings and results. Current columns involve Aquatic Environment, Atmospheric Environment, Environmental Monitoring, Environmental Risk and Assessment, Environmental Biology, Environmental Health and Toxicology, Municipal Solid Waste and Green Chemistry, Soil Environment, Energy and Environment, as well as Other Issues. All the published papers can be browsed on our website ([www.davidpublisher.com](http://www.davidpublisher.com)).

Contribution Requirements:

- 1) Paper must be empirical or theoretical contributions without being published previously;
- 2) All other scholars’ words or remarks as well as their origins must be indicated if quoted;
- 3) English title, abstract and key words should be prerequisite;
- 4) Patterns or forms should conform to the standard listed on our website.

Automatic paper submission system is strongly recommended, while E-mail attachment sent through email at [environmentalAB@hotmail.com](mailto:environmentalAB@hotmail.com); [environmental@davidpublishing.org](mailto:environmental@davidpublishing.org) is still available.

Please visit our website at [www.davidpublisher.com](http://www.davidpublisher.com) for the automatic paper submission systems. Should you have any questions or concerns feel free to contact us.

Best regards,

*Journal of Environmental Science and Engineering*  
David Publishing Company



**Journal of Environmental Science and Engineering A**  
Volume 6, Number 8, August 2017

David Publishing Company  
616 Corporate Way, Suite 2-4876, Valley Cottage, NY 10989, USA  
Tel: 1-323-984-7526, 323-410-1082; Fax: 1-323-984-7374, 323-908-0457  
<http://www.davidpublisher.com>, [www.davidpublisher.org](http://www.davidpublisher.org)  
[environmental@davidpublishing.org](mailto:environmental@davidpublishing.org), [environmental@davidpublishing.com](mailto:environmental@davidpublishing.com)

